

1

Multiple Equilibria

Chemical reactions are initiated by accidental collision of molecules, which have the potential (e.g. sufficient energy) to react with one another to be converted into products:



In living matter it cannot be left to chance whether a reaction happens or not. At exactly the time required the respective compounds must be selected and converted to products with high precision, while at unfavorable times spontaneous reactions must be prevented. An important prerequisite for this selectivity of reactions is the highly specific recognition of the required compound. Therefore, any physiological reaction occurring in the organism is preceded by a specific recognition or binding step between the respective molecule and a distinct *receptor*. The exploration of binding processes is important for understanding biological processes. The receptors can be enzymes, but also non-enzymatic proteins like membrane transport systems, receptors for hormones or neurotransmitters, and nucleic acids. Generally, receptors are macromolecular in nature and thus considerably larger than the efficacious molecules, the *ligands*. For the binding process, however, they must be treated as equivalent partners (unlike for enzyme kinetics, where the enzyme as catalyst does not take part in the reaction).

As a precondition for binding studies specific binding must be established and unspecific association excluded. There exist many reasons for unspecific binding, like hydrophobic or electrostatic interactions (charged ligands can act as counterions for the surplus charges of proteins). A rough indicator for specific binding is the magnitude of the dissociation constant, which is mostly below 10^{-3} M (although there are exceptions, like the binding of H_2O_2 to catalase or glucose to glucose isomerase). Specific binding is characterized by a defined number of binding sites n , which is in stoichiometric relationship to the macromolecule. In contrast, unspecific binding has no defined number of binding sites, and thus the binding process is not saturable. Furthermore, the ligand can be replaced by structural analogs, while different or distantly related compounds are not accepted.

In the following the processes leading to a specific interaction between a ligand and a macromolecule will be described, i.e. how the ligand finds its bind-

ing site and which factors determine the affinity. The essential mechanisms of interaction between ligand and macromolecule are then presented.

1.1 Diffusion

A prerequisite for any reaction of a ligand with a macromolecule is the fact that the partners must find one another. In a free space a particle moves in a straight direction with a kinetic energy of $k_B T/2$, T being the absolute temperature and k_B the Boltzmann constant. According to Einstein's relationship a particle with mass m , moving in a distinct direction with velocity v possesses kinetic energy $mv^2/2$. Combining both relationships Eq. (1.1) follows:

$$v^2 = k_B T/m . \quad (1.1)$$

Accordingly, a macromolecule like the lactate dehydrogenase ($M_r=140\,000$) would move at a rate of 4 m s^{-1} , its substrate lactic acid ($M_r=90.1$) at 170 m s^{-1} , and a water molecule ($M_r=18$) at 370 m s^{-1} . Enzyme and substrate will fly past one another like rifle bullets. In the dense fluid of the cell, however, the moving particles are permanently hampered and deflected from linear movement by countless obstacles: water molecules, ions, metabolites, macromolecules and membranes and, actually, the molecule moves more like a staggering drunkard than in a straight progression. However, this tumbling increases the collision frequency and the probability of distinct molecules meeting one another.

The distance x covered by a molecule in solution within time t in one direction depends on the diffusion coefficient D according to the equation:

$$x^2 = 2Dt . \quad (1.2)$$

The diffusion coefficient is itself a function of the concentration of the diffusing compound, in dilute solutions it can be regarded as constant. It depends on the particle size, the consistency of the fluid and the temperature. For small molecules in water the coefficient is $D=10^{-5}\text{ cm}^2\text{ s}^{-1}$. A cell with the length $1\text{ }\mu\text{m}$ will be passed within 0.5 ms , 1 mm within 500 s , thus, for a thousandfold distance a millionfold time is required. This demonstrates that there exists no 'diffusion velocity', the movement of the molecules is not proportional to time, but to its square root. A diffusing molecule does not remember its previous position, it does not strive systematically for new spaces but searches new regions randomly in undirected movement. As an example, a 10 cm high saccharose gradient, used in ultracentrifugation for separation and molecular mass determination of macromolecules, has a life-span of about four months, taking $D=5\times 10^{-6}\text{ cm}^2\text{ s}^{-1}$ for saccharose. The tendency of the gradient to equalize its concentration is considerably low.

Equation (1.2) describes the one-dimensional diffusion of a molecule. For diffusion in a three-dimensional space over a distance r the diffusion into the three space directions x , y and z is assumed to be independent of each other:

$$r^2 = x^2 + y^2 + z^2 = 6Dt . \quad (1.3)$$

Mere meeting of ligand and macromolecule is not sufficient to accomplish specific binding, rather the ligand must locate the binding site on the macromolecule. This is realized by translocation of the ligand volume $4\pi R^3/3$ by the relevant distance of its own radius R . After a time t_x the molecule has searched (according to Eq. (1.3) for $r=R$) a volume of:

$$\frac{6Dt_x}{R^2} \cdot \frac{4\pi R^3}{3} = 8\pi DRt_x . \quad (1.4)$$

The volume searched per time unit is $8\pi DR$, the probability of collision for a certain particle in solution is proportional to the diffusion coefficient and the particle radius.

At the start of a reaction $A+B \rightarrow P$ both participants are equally distributed in solution. Within a short time, molecules of one type, e.g. B, become depleted in the vicinity of the molecule of the other type (A) not yet converted, so that a concentration gradient will be formed. Consequently, a net flow Φ of B-molecules occurs in the direction of the A-molecules located at a distance r ,

$$\Phi = \frac{dn}{dt} = DF \frac{dc}{dr} , \quad (1.5)$$

n is the net surplus of molecules passing through an area F within time t , c is the concentration of B-molecules located at a distance r from the A-molecules. This relationship in its general form is known as *Fick's First Law of Diffusion*. In our example of a reaction of two reactants, F has the dimension of a spherical surface with the radius r . Eq. (1.5) then changes into:

$$\left(\frac{dc}{dr}\right)_r = \frac{\Phi}{4\pi r^2 D'} \quad (1.6)$$

D' is the diffusion coefficient for the relative diffusion of the reactive molecules. Integration of Eq. (1.6) yields:

$$c_r = c_\infty - \frac{\Phi}{4\pi r D'} \quad (1.7)$$

where c_r is the concentration of B-molecules at the distance r and c_∞ the concentration at infinite distance from the A-molecules. The last corresponds approximately to the average concentration of B-molecules. The net flow Φ is proportional to the reaction rate and that is again proportional to the average concentration c of those B-molecules just in collision with the A-molecules, r_{A+B} being the sum of the radii of an A- and a B-molecule:

$$\Phi = kc_{r_{A+B}} . \quad (1.8)$$

where k is the rate constant of the reaction in the steady-state, where c_r becomes equal to $c_{r_{A+B}}$ and r equal to r_{A+B} . Inserted into Eq. (1.7), this becomes:

$$c_{r_{A+B}} = \frac{c_\infty}{1 + \frac{k}{4\pi r_{A+B} D'}} \quad (1.9)$$

The net flow under steady-state conditions is:

$$\Phi = k_a c_\infty \quad (1.10)$$

where k_a is the relevant association rate constant. Equations (1.8)–(1.10) may thus be rewritten:

$$\frac{1}{k_a} = \frac{1}{4\pi r_{A+B} D'} + \frac{1}{k} \quad (1.11)$$

This relation becomes linear in a graph plotting $1/k_a$ against the viscosity η of the solution as, according to the *Einstein-Sutherland Equation*, the diffusion coefficient at infinite dilution D_0 is inversely proportional to the friction coefficient f and that again is directly proportional to the viscosity η .

$$D_0 = \frac{k_B T}{f} = \frac{k_B T}{6\pi\eta r} \quad (1.12)$$

$1/k$ is the ordinate intercept. In the case of $k \gg 4\pi r_{A+B} D'$ the intercept is placed near the coordinate base, it becomes:

$$k_a = 4\pi r_{A+B} D' \quad (1.13)$$

This borderline relationship is known as the *Smoluchowski limit* for translating diffusion, the reaction is *diffusion-controlled*. In contrast to this, in *reaction-controlled* reactions the step following diffusion, i.e. the substrate turnover, determines the rate. A depletion zone emerges around the enzyme molecule, as substrate molecules are not replaced fast enough. A *diffusion-limited dissociation* occurs, if the dissociation of the product limits the reaction. Viewing two equally reactive spheres with radii r_A and r_B and diffusion coefficients D_A and D_B , we obtain for Eq. (1.13):

$$k_a = 4\pi r_{A+B} D' = 4\pi(r_A + r_B)(D_A + D_B) \quad (1.14)$$

By inserting Eq. (1.12) and with the approximation $r_A = r_B$ and with $D_0 = D_A = D_B$ we obtain:

$$k_a = \frac{8k_B T}{3\eta} \quad (1.15)$$

Thus the association rate constants for diffusion-controlled reactions are in the range 10^9 – $10^{10} \text{ M}^{-1} \text{ s}^{-1}$.

Uniform values should be obtained if the rate constants are exclusively determined by diffusion. In reality, however, the values of the rate constants of diffusion-controlled reactions of macromolecules vary within a range of more than five orders of magnitude. The reason for this variation is that, for successful binding of the ligand, random collision with the macromolecule is not sufficient. Both molecules must be in a favorable position to each other. This causes a considerable retardation of the binding process. On the other hand, attracting forces could facilitate the interaction and direct the ligands towards their proper orientation. Under such conditions rate constants can even surpass the values of mere diffusion control. Quantitative recording of such influences is difficult as they depend on the specific structures of both the macromolecule and the ligand. Theories have been developed to establish general rules for ligand binding.

Ligand approach a macromolecule at a rate according to Eq. (1.13), but only those meeting the correct site in the right orientation will react. If the binding site is regarded as a circular area, forming an angle α with the center of the macromolecule (see Fig. 1.1), the association rate constant of Eq. (1.13) will be reduced by the sine of that angle:

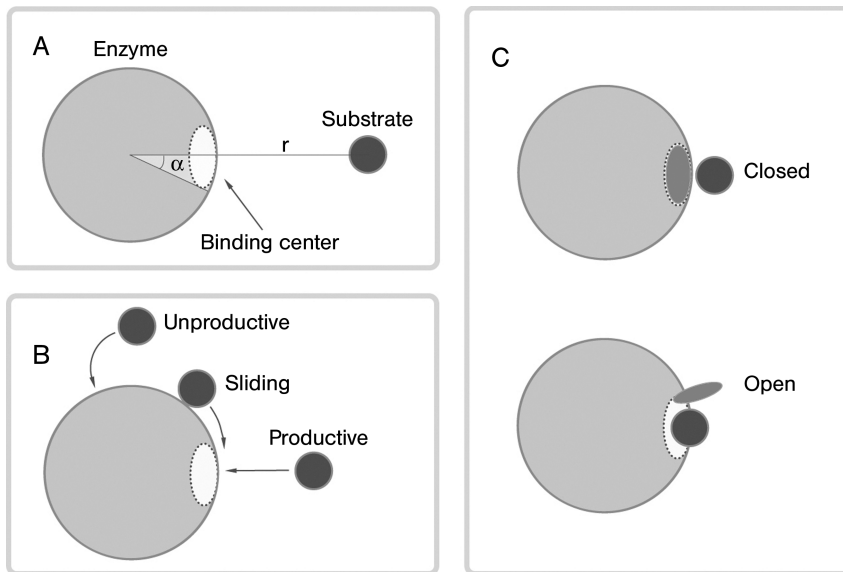


Fig. 1.1 Schematic illustration of the interaction of a substrate molecule with its binding site on the enzyme (A). B, productive and unproductive binding, sliding of the ligand along the surface; C, gating.

$$k_a = 4\pi r_{A+B} D' \sin \alpha . \quad (1.16)$$

The necessity of appropriate orientation between ligand and binding site should be considered by the introduction of a suitable factor, depending on the nature of the reactive groups involved. It is also suggested that the ligand may associate unspecifically to the surface of the macromolecule, where it dissociates in a two-dimensional diffusion to find the binding site (*sliding model*; Berg, 1985, Fig. 1.1 B). Such unspecific binding, however, is not able to distinguish between the specific ligand and other metabolites which may also bind and impede the two-dimensional diffusion. The *gating model* (Fig. 1.1 C) assumes the binding site to be opened and closed like a gate by changing the conformation of the protein, thus modulating the accessibility for the ligand (McCammion and Northrup 1981).

A basic limit for the association rate constant for the enzyme substrate is the quotient from the catalytic constant k_{cat} and the Michaelis constant K_m (cf. Section 2.2.1):

$$\frac{k_{\text{cat}}}{K_m} = \frac{k_{\text{cat}}k_1}{k_{-1} + k_2} \quad (1.17)$$

frequently around $10^8 \text{ M}^{-1} \text{ s}^{-1}$ for a diffusion-controlled reaction. For most enzyme reactions the reaction rate is determined more by the non-covalent steps during substrate binding and product dissociation rather than by the cleavage of bounds.

1.2

Interaction between Macromolecules and Ligands

1.2.1

Binding Constants

Binding of a ligand A to a macromolecule E



is described with the law of mass action, applying the association constant K_a :

$$K_a = \frac{k_1}{k_{-1}} = \frac{[\text{EA}]}{[\text{A}][\text{E}]} \quad (1.19 \text{ a})$$

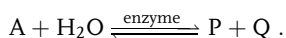
or its reciprocal value, the dissociation constant K_d :

$$K_d = \frac{k_{-1}}{k_1} = \frac{[\text{A}][\text{E}]}{[\text{EA}]} \quad (1.19 \text{ b})$$

Both notations are used, the association constant more frequently for the treatment of equilibria, the dissociation constant for enzyme kinetics. Here the dissociation

constant will be employed throughout. The association constant has the dimension of a reciprocal concentration (M^{-1}), the higher the numerical value, the higher the affinity. Conversely, dissociation constants possess the dimension of a concentration (M) and lower values indicate stronger binding. Eqs. (1.19 a, b) are not quite correct, in the place of concentrations c (e.g. [A]) activities $a=fc$ should be used. Since activity coefficients f approach one in very dilute solutions they can be disregarded for enzyme reactions.

If one reaction component is present in such a large excess that its concentration change during the reaction can be neglected, the absolute concentration can be included in the constant. This applies especially for water, if it takes part in the reaction, e.g. in hydrolytic processes:



As a solvent, with a concentration of 55.56 mol l^{-1} , water exceeds by far the nano- to millimolar amounts of the other components in an enzyme assay and any change in its concentration will hardly be detectable. Therefore, a binding constant for water cannot be determined and the reaction will be treated as if water is not involved:

$$K'_d = \frac{[A][H_2O]}{[P][Q]} = K_d[H_2O]; \quad K_d = \frac{[A]}{[P][Q]} .$$

Hydrogen ions, frequently involved in enzyme reactions, are treated in a similar manner. An apparent dissociation constant is defined:

$$K_{\text{app}} = K_d[H^+] .$$

Contrary to genuine equilibrium constants this constant is dependent on the pH value in the solution.

1.2.2

Macromolecules with One Binding Site

To determine the binding constants for a distinct system the mass action law (Eq. (1.19)) can be applied. However, the terms required for solution of the equation, the concentrations of the free macromolecule [E], the free substrate [A] and the enzyme-substrate complex [EA], are unknown. Only the total amounts of macromolecule $[E]_0$ and of ligand $[A]_0$ added to the reaction are known. They separate into free and bound components according to the mass conservation principle:

$$[E]_0 = [E] + [EA] \quad (1.20)$$

$$[A]_0 = [A] + [EA] . \quad (1.21)$$

Binding experiments yield the portion of the ligand bound to the macromolecule $[A]_{\text{bound}}$ (see Chapter 3). In the simple reaction with only one ligand bind-

ing to a macromolecule (Eq. (1.18)) $[A]_{\text{bound}}$ is equal to $[EA]$. Inserting Eq. (1.20) into Eq. (1.19b) eliminates the free macromolecule concentration $[E]$:

$$[A]_{\text{bound}} = \frac{[E]_0 [A]}{K_d + [A]} \quad (1.22)$$

This equation describes the binding of a ligand to a macromolecule with one binding site. It will be discussed in detail in the following section together with the analogous Eq. (1.23) for macromolecules with several identical binding sites.

1.3

Macromolecules with Identical Independent Binding Sites

1.3.1

General Binding Equation

Most proteins and enzymes found in living organisms are composed of more than one, mostly identical, subunit. For reasons of symmetry it can be taken that each of these subunits carries one identical binding site for the ligand, so that the number n of binding sites equals the number of subunits. This is a plausible assumption, but it must be stated that, in the strict sense, identity means equality of binding constants. If affinities of binding sites located on non-identical subunits are the same by chance, or if a single subunit possesses more than one binding site with similar binding constants (e.g. due to gene duplication), this will not be differentiated by binding analysis and requires additional experiments.

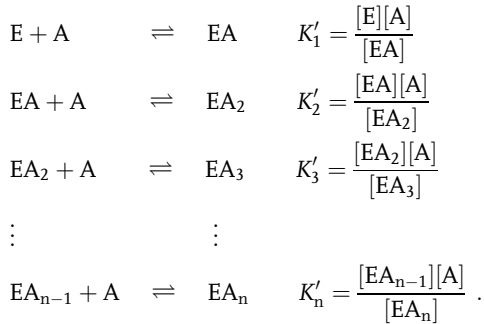
Binding of a ligand to identical sites on the same macromolecule can occur independently, otherwise the first bound ligand can influence the following binding steps. Such influences will be considered in Section 1.5, while here only independent binding is considered. Such binding processes are principally described by Eq. (1.22), since it should make no essential difference whether the binding occurs at a macromolecule with only one binding site, or whether n sites are gathered on the same macromolecule. If $[F]_0 = n[E]_0$ is assumed to be the total amount of binding sites, this can replace $[E]_0$ in Eq. (1.22):

$$[A]_{\text{bound}} = \frac{[F]_0 [A]}{K_d + [A]} = \frac{n [E]_0 [A]}{K_d + [A]} \quad (1.23)$$

The number of binding sites is indicated in the numerator, but as a further difference it must be considered, that $[A]_{\text{bound}}$ can no longer be equated with $[EA]$, but comprises all partially saturated forms of the macromolecule:

$$[A]_{\text{bound}} = [EA] + 2 [EA_2] + 3 [EA_3] + \dots + n [EA_n] \quad (1.24)$$

In fact the macromolecule will be saturated stepwise:

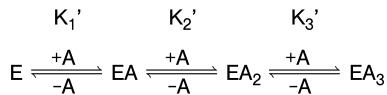


Each step has its own dissociation constant. For independent binding all individual dissociation constants may be taken as equal and Eq. (1.23) will be obtained. Although these considerations lead to the correct binding equation, the derivation was simplified. The correct derivation, which is much more complicated, is given in Box 1.1.

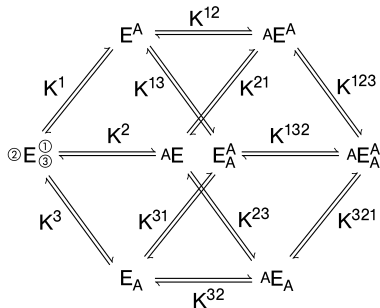
Box 1.1 Derivation of the General Binding Equation

The dissociation constants of the individual binding steps are called *macroscopic* dissociation constants K' , in contrast to *microscopic* (or *intrinsic*) binding constants K for binding to the individual sites of the macromolecule.

Macroscopic binding constants



Microscopic binding constants



Scheme 1. Macroscopic and microscopic binding constants of a macromolecule with three identical binding sites. The E-form at the left in the lower scheme shows the relative orientation and the denomination of the binding sites. The constants are designated according to the sequence of occupation, the last figure indicating the actual occupation.

This is demonstrated in Scheme 1 for a macromolecule with three binding sites. The first binding step has one macroscopic dissociation constant K'_1 , but three microscopic dissociation constants, designated as K^1 , K^2 , and K^3 , according to the numbers of the binding sites $2E_3^1$. Therefore, one ligand binding to the macromolecule can choose between three binding sites and, consequently, three different macromolecule species can be formed. For the second binding step three forms are also possible, but there are six ways to obtain these species, accordingly there exist six microscopic dissociation constants (K^{12} etc.). From these three forms three equilibria characterized by three microscopic binding constants (K^{123} etc.) lead to the one fully saturated macromolecule form. Obviously the complete binding process is described by three macroscopic and twelve microscopic dissociation constants (Scheme 1). The relationship between both types of constants can be established by applying the respective mass action laws. The macroscopic dissociation constant of the first binding step is defined as:

$$K'_1 = \frac{[E][A]}{[EA]} = \frac{[E][A]}{[E^A] + [{}_A E] + [E_A]} .$$

The microscopic binding constants are used to replace the individual macromolecule forms

$$\begin{aligned} K^1 &= \frac{[E][A]}{[E^A]} ; & [E^A] &= \frac{[E][A]}{K^1} \\ K^2 &= \frac{[E][A]}{[{}_A E]} ; & [{}_A E] &= \frac{[E][A]}{K^2} \\ K^3 &= \frac{[E][A]}{[E_A]} ; & [E_A] &= \frac{[E][A]}{K^3} \\ K'_1 &= \frac{1}{\frac{1}{K^1} + \frac{1}{K^2} + \frac{1}{K^3}} . \end{aligned}$$

If the three binding sites are identical, the microscopic constants can be equalized, $K^1=K^2=K^3=K$, and both types of constants are related as $K'=K/3$.

Correspondingly, the second binding step is:

$$\begin{aligned} K'_2 &= \frac{[EA][A]}{[EA_2]} = \frac{([E^A] + [{}_A E] + [E_A])[A]}{[{}_A E^A] + [E^A] + [{}_A E_A]} \\ K^{12} &= \frac{[E^A][A]}{[{}_A E^A]} ; & [{}_A E^A] &= \frac{[E^A][A]}{K^{12}} \quad \text{etc., hence} \\ K'_2 &= \frac{K^{13} K^{21} K^{23} + K^{12} K^{13} K^{23} + K^{13} K^{21} K^{32}}{K^{13} K^{23} + K^{12} K^{23} + K^{13} K^{21}} . \end{aligned}$$

For $K^{12} = K^{13} = \dots = K$ results $K'_2 = K$.

The third binding step is:

$$K'_3 = \frac{[\text{EA}_2][\text{A}]}{[\text{EA}_3]} = \frac{([\text{A} \text{E}^{\text{A}}] + [\text{E}^{\text{A}}_{\text{A}}] + [\text{A} \text{E}_{\text{A}}])[\text{A}]}{[\text{A} \text{E}^{\text{A}}_{\text{A}}]},$$

$$K^{123} = \frac{[\text{A} \text{E}^{\text{A}}][\text{A}]}{[\text{A} \text{E}^{\text{A}}_{\text{A}}]}; \quad [\text{A} \text{E}^{\text{A}}] = \frac{K^{123}[\text{A} \text{E}^{\text{A}}_{\text{A}}]}{[\text{A}]} \text{ etc.}$$

For $K^{123} = K^{132} = \dots = K$ results $K'_3 = 3K$.

Even if all microscopic dissociation constants are identical, they differ from the macroscopic ones and there are differences between each binding step. The general relationship between both types of dissociation constants for n binding sites is

$$K'_d = K_d \frac{i}{n - i + 1}, \quad (2)$$

i representing the respective binding step. Ligands occupying stepwise a macromolecule with identical sites have Ω possibilities of orientation, depending on the respective binding step i :

$$\Omega = \frac{n!}{(n - i)!i!} \quad (3)$$

For the derivation of the general binding equation a saturation function r is defined as the quotient from the portion of bound ligand to the total amount of the macromolecule:

$$r = \frac{[\text{A}]_{\text{bound}}}{[\text{E}]_0} = \frac{[\text{EA}] + 2[\text{EA}_2] + 3[\text{EA}_3] + \dots + n[\text{EA}_n]}{[\text{E}] + [\text{EA}] + [\text{EA}_2] + [\text{EA}_3] + \dots + [\text{EA}_n]}. \quad (4)$$

The concentrations of the individual macromolecule forms are not accessible experimentally and are replaced by the macroscopic dissociation constants:

$$K'_1 = \frac{[\text{E}][\text{A}]}{[\text{EA}]}; \quad [\text{EA}] = \frac{[\text{E}][\text{A}]}{K'_1}$$

$$K'_2 = \frac{[\text{EA}][\text{A}]}{[\text{EA}_2]}; \quad [\text{EA}_2] = \frac{[\text{EA}][\text{A}]}{K'_2} = \frac{[\text{E}][\text{A}]^2}{K'_1 K'_2}$$

$$K'_3 = \frac{[\text{EA}_2][\text{A}]}{[\text{EA}_3]}; \quad [\text{EA}_3] = \frac{[\text{EA}_2][\text{A}]}{K'_3} = \frac{[\text{E}][\text{A}]^3}{K'_1 K'_2 K'_3}$$

$$\vdots \quad \quad \quad \vdots \quad \quad \quad \vdots$$

$$K'_n = \frac{[\text{EA}_{n-1}][\text{A}]}{[\text{EA}_n]}; \quad [\text{EA}_n] = \frac{[\text{EA}_{n-1}][\text{A}]}{K'_n} = \frac{[\text{E}][\text{A}]^n}{K'_1 K'_2 K'_3 \dots K'_n}.$$

Thus evolves:

$$\begin{aligned}
 r &= \frac{\frac{[A]}{K'} + \frac{2[A]^2}{K'_1 K'_2} + \frac{3[A]^3}{K'_1 K'_2 K'_3} + \dots + \frac{n[A]^n}{K'_1 K'_2 K'_3 \dots K'_n}}{1 + \frac{[A]}{K'_1} + \frac{[A]^2}{K'_1 K'_2} + \frac{[A]^3}{K'_1 K'_2 K'_3} + \dots + \frac{[A]^n}{K'_1 K'_2 K'_3 \dots K'_n}} \\
 &= \frac{\sum_{i=1}^n \frac{i[A]^i}{\left(\prod_{j=1}^i K'_j\right)}}{1 + \sum_{i=1}^n \frac{[A]^i}{\prod_{j=1}^i K'_j}}. \tag{5}
 \end{aligned}$$

In the case of independent identical binding sites the macroscopic binding constants of the individual binding steps according to Eq. (2) are replaced by a uniform microscopic constant K_d :

$$r = \frac{\sum_{i=1}^n i \left(\prod_{j=1}^i \frac{n-j+1}{j} \right) \left(\frac{[A]}{K_d} \right)^i}{1 + \sum_{i=1}^n \left(\prod_{j=1}^i \frac{n-j+1}{j} \right) \left(\frac{[A]}{K_d} \right)^i}. \tag{6}$$

The product terms of the numerator and denominator are binomial coefficients, which can be converted as follows:

$$\binom{n}{i} = \left(\frac{n!}{i!(n-i)!} \right),$$

so that Eq. (6) may be written in the form:

$$r = \frac{\sum_{i=1}^n i \binom{n}{i} \left(\frac{[A]}{K_d} \right)^i}{1 + \sum_{i=1}^n \binom{n}{i} \left(\frac{[A]}{K_d} \right)^i}.$$

Applying the binomial rule, the denominator can be converted as $(1+[A]/K_d)^n$. For the numerator the derived binomial rule applies:

$$r = \frac{n \left(\frac{[A]}{K_d} \right) \left(1 + \frac{[A]}{K_d} \right)^{n-1}}{\left(1 + \frac{[A]}{K_d} \right)^n}.$$

By reduction the already known form of the binding equation (Eq. (1.23)) will be achieved:

$$r = \frac{[A]_{\text{bound}}}{[E]_0} = \frac{n[A]}{K_d + [A]}. \tag{7}$$

Irvin Langmuir developed such an equation in 1916 for the adsorption of gases to solid surfaces and, therefore, the authorship of this equation is ascribed to him, although Adrian J. Brown and Victor Henri had already developed a similar equation in 1900, which was examined in detail by Leonor Michaelis and Maud Menten in 1913. This *Michaelis-Menten equation*, already exhibiting some modifications in comparison to Eq. (1.23), is of general importance for enzyme kinetics (see Section 2.2.1).

Equation (1.23) describes the relationship between the free and the bound ligand. By successive increase of the free ligand a saturation curve will be obtained (Fig. 1.2A), which follows mathematically the function of a right-angle hyperbola (this will be explained in Section 2.3.1, Box 2.1). At extremely high concentrations of A ($[A] \rightarrow \infty$) K_d in the denominator of Eq. (1.23) can be ignored and the curve approaches n , the number of binding sites. At the position where the free ligand concentration equals the value of the dissociation constant, $[A]=K_d$, $r=n/2$, according to Eq. (1.23). In this manner the K_d value can be determined from half saturation. Thus both the dissociation constant and the number of binding sites can be obtained from this saturation curve (Fig. 1.2A).

There exist three, principally equivalent modes of plotting binding data. The amount of bound ligand $[A]_{\text{bound}}$ obtained from the experiment can be plotted directly against the free ligand concentration $[A]$. Saturation will be reached at

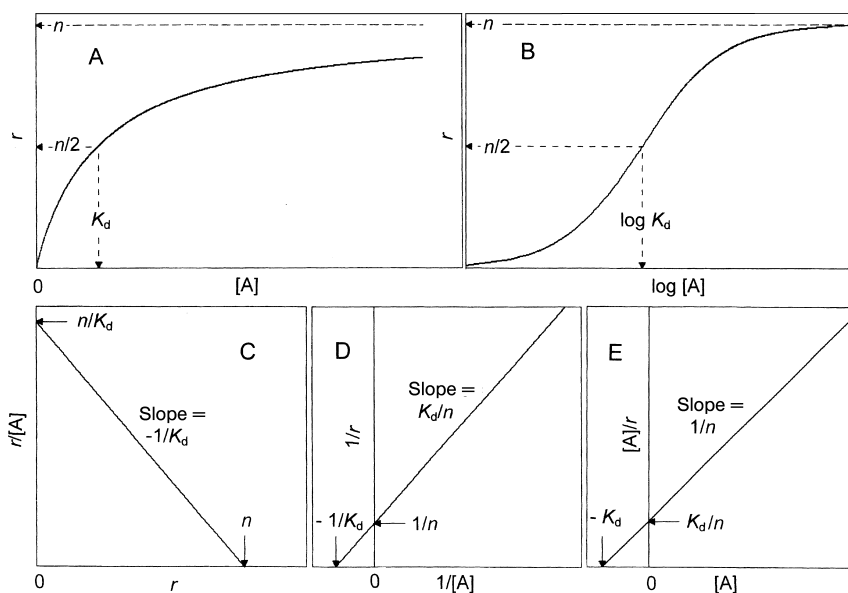


Fig. 1.2 Modes of representation of binding data. (A) Direct plot; (B) semi-logarithmic plot; (C) Scatchard plot; (D) double-reciprocal plot; (E) Hanes plot.

$n[E]_0$. It is more convenient to take the saturation function r by division of $[A]_{\text{bound}}$ by $[E]_0$, as discussed already. If r is further divided by n , the function \bar{Y} results:

$$\bar{Y} = \frac{[A]_{\text{bound}}}{n[E]_0} = \frac{[A]}{K_d + [A]} . \quad (1.23 \text{ a})$$

In this case the value of the saturation becomes 1. The function \bar{Y} is used if different mechanisms are compared theoretically (without defining n) or, experimentally, where the portion of bound ligand is not directly known, as in spectroscopic titrations (see Section 1.3.2.2).

1.3.2

Graphic Representations of the Binding Equation

1.3.2.1 Direct and Linear Diagrams

Generally binding studies should yield 3 kinds of information:

- The affinity of the macromolecule for the ligand, represented by the value of the dissociation constant K_d .
- The number of binding sites n .
- The respective binding mechanism.

The goal of graphic representations is to obtain this information in a clear, unambiguous manner. There exist different kinds of graphic representations and it must be decided which will be the most appropriate for the respective experimental data. Usually the data will be represented in a variety of plots because special aspects will become more obvious in one type than in another, although, as a rule, missing information cannot be recalled by any representation.

The direct representation of binding data has already been discussed (Fig. 1.2A). This is always recommended as a primary step, since the data suffer no distortion, especially with respect to the error distribution, due to recalculations, as in linear diagrams. A difficulty is the treatment of saturation, which is mostly underestimated, as saturation is actually reached at infinity. It must be considered that experimentally a continuous curve is not obtained, rather, a scattering set of data points. Thus determination of n , and also of K_d , depending on half saturation, may become difficult. Non-linear regression analysis improves the analysis.

Besides the problems of determination of the constants, the detection of possible alternative binding mechanisms (which will be discussed later) is more difficult with the direct, non-linear plot, because weak deviations from the normal function will easily be hidden behind the data scatter. Linear representations partly avoid such disadvantages but they reveal other limitations.

An alternative non-linear representation is the *semi-logarithmic plotting* of the saturation function r against $\log [A]$. This diagram is recommended especially when larger concentration ranges are covered, which cannot be resolved complete-

ly in the direct plot. Sigmoidal curves are obtained in the semi-logarithmic representation (Fig. 1.2B) and the logarithm of K_d is obtained from half saturation.

The similarity of the binding equation with the Michaelis-Menten equation holds also for the linearization methods, which will be discussed in detail in Section 2.3.1. Accordingly, there exist three simple linear transformations of the equations. One is the *double-reciprocal plot*, ascribed to Klotz (1946) (although he was not the original author; moreover, equivalent plots are designated differently for binding and kinetic treatments as will be discussed in Section 2.3.1.3). The reverse form of Eq. (1.23) is:

$$\frac{1}{r} = \frac{1}{n} + \frac{K_d}{n[A]}. \quad (1.25)$$

Plotting $1/r$ against $1/[A]$ should result in a straight line, intercepting the ordinate at $1/n$ and the abscissa at $-1/K_d$. Therefore, both constants can easily be obtained by extrapolation (Fig. 1.2D). Alternative mechanisms show characteristic deviations from linearity. The double-reciprocal plot has the advantage of separation of the variables (in contrast to the other two linear diagrams), however, due to the reciprocal entry, strong distortions of the error limits result, being compressed to the high and expanded to the low ligand range. Linear regression is not applicable and especially the determination of n at the ordinate intercept often becomes dubious with scattering data.

Because n is an important value, the plot of *Scatchard* (1949) is preferred for the analysis of binding data. It is derived from Eq. (1.25) by multiplying by m/K_d :

$$\frac{r}{[A]} = \frac{n}{K_d} - \frac{r}{K_d}. \quad (1.26)$$

Plotting $r/[A]$ versus r results in a straight line intersecting the abscissa at n and the ordinate at n/K_d (Fig. 1.2C). In this diagram also the error limits do not remain constant, but increase towards high ligand concentrations, but the effect is lower than with the double-reciprocal diagram and linear regression is often applied. Although the variables are not separated, this is the most reliable linear diagram.

A third diagram is obtained by multiplying Eq. (1.25) by $[A]$:

$$\frac{[A]}{r} = \frac{[A]}{n} + \frac{K_d}{n}. \quad (1.27)$$

This diagram, known in enzyme kinetics as the *Hanes plot*, is seldom used for binding analysis. By plotting $[A]/r$ versus $[A]$, K_d/n follows from the ordinate and $-K_d$ from the abscissa intercept (Fig. 1.2E). An advantage of this representation are the nearly constant error limits.

1.3.2.2 Analysis of Binding Data from Spectroscopic Titrations

Although methods for determination of binding are discussed later (see Chapter 3.4), theoretical aspects of the analysis will be discussed here. Spectroscopic titrations are convenient methods to study binding processes but the data need a special treatment as the diagrams discussed so far cannot be applied directly. The main difference to other binding methods is that the share of the free ligand $[A]$ cannot be obtained directly by experiment and also the share of bound ligand results only as a relative spectral change, not as a molar concentration. The experimental procedure is usually the addition of increasing amounts of the ligand to a constant amount of the macromolecule in a photometric cuvette and the spectral change is recorded in dependence on the ligand concentration. Only the total amount of the added ligand $[A]_0$ is known, while for a plot as shown in Fig. 1.2A the free ligand concentration is required. In principle the same problem exists in enzyme kinetics where also the total substrate concentration is taken. However, because of the very low ('catalytic') enzyme concentrations the amounts of total and free ligand can be equated. This is not possible with binding measurements, where the macromolecule will be present in high concentrations to produce a detectable signal. Therefore, direct representation of the spectral change against $[A]_0$, as obtained from the experiment (*titration curve*), cannot be evaluated as discussed in Section 1.3.2.1 with K_d at half saturation. There exist different approaches to the evaluation of such titration curves, one of them, the Dixon plot, will be discussed in Section 2.3.1.1.

For direct evaluation of titration curves it can be assumed that in the low concentration range of the ligand for $[A]_0 < [E]_0$ nearly all ligand added will bind to the macromolecule, thus $[A]_0 \sim [A]_{\text{bound}}$ and no free ligand appears. Under these conditions a linear relation between the added ligand and $[A]_{\text{bound}}$ will occur, discernible by a linear increase in the spectral signal in the low ligand range. A tangent at this part of the titration curve represents the share of the bound ligand throughout (Fig. 1.3 A). At higher ligand concentration only part of the ligand will bind and the remaining free ligand causes deviation of the saturation curve from the initial tangent. The spectral signal still increases upon further addition of ligand as long as free binding sites are available, but the increase will cease when all sites become occupied. Now the saturation curve tends to a saturation plateau, which can be indicated by an asymptotic line (also here it must be considered that saturation occurs actually at infinity). The optical signal at the position of the asymptotic line corresponds to the amount of ligand bound at saturation, and thus to all available binding sites $n[E]_0$. The concentration of $n[E]_0$ can be obtained directly from the abscissa coordinate of the intersection point of both the initial tangent and the asymptote (see Fig. 1.3 A). The relative values of the optical signal at the ordinate can be converted to \bar{Y} values, setting the saturation equal to $\bar{Y}=1$. The total amount of ligand $[A]_0$ is the sum of free and bound ligand. Both shares can be obtained directly by a parallel line to the abscissa at any point of the curve. The distance from the ordinate axes to the tangent (abscissa coordinate) is $[A]_{\text{bound}}$ and that from there to the titration curve is $[A]$. In this manner all measured data can be converted into these two values, with the exception of the points in the low ligand range, which are used for

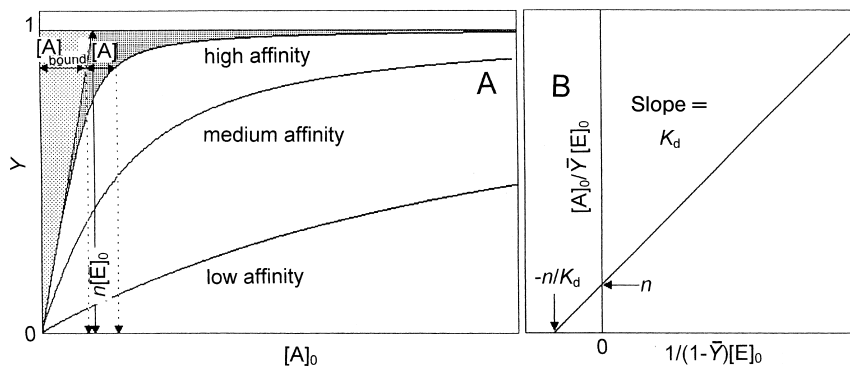


Fig. 1.3 Evaluation of spectroscopic titrations. (A) Direct plotting, (B) Stockell plot.

aligning the tangent. With the knowledge of $[A]_{\text{bound}}$ and $[A]$, the conventional diagrams described in Section 1.3.2.1 and the respective evaluation of the constants can be performed. The severe disadvantage of this procedure is that it depends essentially on the alignment of the tangent. If there is a larger scatter, or if the assumption that at low ligand concentrations all ligand will be bound is not valid, the alignment will become incorrect. This is especially the case with low affinity binding, where there is a tendency to align the tangent too flat. Principally, the higher the affinity, the more the experimental curve approaches the two asymptotic lines, both these lines represent the case of infinite high affinity.

To circumvent the uncertainty of the initial tangent, the titration curve can be directly linearized according to a procedure suggested by *Stockell* (1959), where the free ligand concentration in Eq. (1.23) is replaced by $[A]_0$. The spectral signal is converted into values for \bar{Y} , saturation being defined as $\bar{Y}=1$. To derive a linear relationship $r = n\bar{Y} = n[EA]/[E]_0$ is inserted into Eq. (1.25), and $[A]_{\text{bound}} = n[EA]$:

$$\frac{1}{\bar{Y}} = 1 + \frac{K_d}{[A]_0 - n[EA]} = 1 + \frac{K_d}{[A]_0 - n\bar{Y}[E]_0}.$$

Transformation to

$$\frac{[A]_0}{\bar{Y}} - [A]_0 = n[E]_0(1 - \bar{Y}) + K_d$$

results in:

$$\frac{[A]_0}{[E]_0\bar{Y}} = \frac{K_d}{[E]_0(1 - \bar{Y})} + n. \quad (1.28)$$

In this diagram (Fig. 1.3 B) a straight line should result and n and K_d can be obtained from the ordinate and abscissa intercepts, respectively. There still remains the uncertainty of the saturation asymptote, which is required for the definition of $\bar{Y}=1$. Therefore, the measurements must be extended far into the

saturation range. This plot is very sensitive even for weak deviations from the theoretical function and a wrong saturation value may distort the whole curve. For this reason the Stockell plot is more difficult to interpret compared with the direct linearization methods of the binding equation in the case of alternative mechanisms or artificial influences.

For the evaluation procedure of *Job* (1928) the total concentrations of ligand and macromolecule are kept constant and only the molar proportions of both components are altered. X is the mol fraction of the macromolecule and Y that of the ligand, $X + Y = 1$. This is plotted against $[A]_{\text{bound}}$, determined, for example, by an optical signal or the enzyme activity. A curve results as shown in Fig. 1.4 and tangents are aligned at the positions $X=0$ and $Y=0$. Their common intercept has the value:

$$\frac{Y_i}{X_i} = \frac{K_d + nc_0}{K_d + c_0} \quad (1.29)$$

X_i and Y_i are the mol fractions of macromolecule and ligand at the intercept, $c_0 = [E]_0 + [A]_0$ is the (constant) sum of the total concentrations of macromolecule and ligand. For $c_0 \gg K_d$ then $X_i/Y_i = n$. Here the stoichiometry of the binding can be taken from the ratios of the mol fractions at the tangent intercept. For $c_0 \ll K_d$ then $X_i/Y_i = 1$, the curve takes a symmetrical shape and the intercept always has the value 1, irrespective of the actual number of binding sites. This is a disadvantage of the Job plot. It can be circumvented as long as the sum of the macromolecule and ligand concentrations is higher than the value of the dissociation constant. If n is known, K_d can be calculated from Eq. (1.29), whereby the condition $c_0 \sim K_d$ should be regarded. K_d can also be obtained from the maximum of the curve in Fig. 1.4 according to

$$K_d = \frac{(an + a - n)^2 c_0}{4an} \quad (1.30)$$

Here a represents the ratio of the actual measured value at the maximum, M_m , to the saturation value, M_∞ .

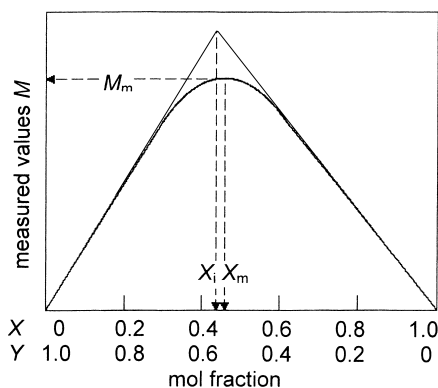


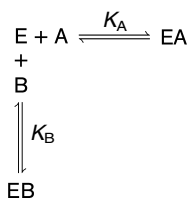
Fig. 1.4 Job plot for the evaluation of binding data.

1.3.3

Binding of Different Ligands, Competition

Due to the high binding specificity of proteins and especially of enzymes, usually only the physiological ligand or the enzyme substrate will be able to bind, while all other metabolites will be excluded. However, this selection cannot be absolute and compounds with high structural homology to the ligand may also be accepted. Knowing the configuration of the binding site or the active center such analogs can be designed and may, sometimes, bind even with higher affinity than the natural ligand. Such analogs may induce similar effects as the ligand, but mostly they are inactive and block the binding site for the native ligand, preventing its action and revealing an antagonistic effect. This *competition* for a distinct binding site of two or more compounds is a valuable tool to investigate specific binding, the action of drugs depends frequently on the antagonistic effect (e.g. β -receptor blocker). Competition is also a valuable tool in cases where binding of the ligand is difficult to detect, e.g. because of the lack of a measurable signal. In such cases a detectable second, e.g. fluorescent-labeled, ligand is applied. At first the binding characteristic and the dissociation constant of the labeled ligand is determined, thereafter the measurements are repeated in the presence of constant amounts of the unlabeled ligand and the dissociation constant for this ligand is obtained as described in the following.

The competition can be described by the scheme:



The binding affinities are expressed by the dissociation constants K_A and K_B for both compounds:

$$K_A = \frac{[\text{E}][\text{A}]}{[\text{EA}]} \quad \text{and} \quad K_B = \frac{[\text{E}][\text{B}]}{[\text{EB}]} \quad (1.31 \text{ a})$$

The total amount of the macromolecule is

$$[\text{E}]_0 = [\text{E}] + [\text{EA}] + [\text{EB}] .$$

$[\text{E}]$ and $[\text{EB}]$ are replaced by K_A and K_B in Eq. (1.31 a):

$$[\text{E}]_0 = \frac{K_A[\text{EA}]}{[\text{A}]} \left(1 + \frac{[\text{B}]}{K_B} \right) + [\text{EA}] .$$

By conversion the following expression for [EA] is obtained:

$$[\text{EA}] = \frac{[\text{E}]_0[\text{A}]}{[\text{A}] + K_A \left(1 + \frac{[\text{B}]}{K_B}\right)} .$$

For a macromolecule with n binding sites Eq. (1.32) results, as discussed already for Eq. (1.23):

$$r = \frac{n[\text{A}]}{[\text{A}] + K_A \left(1 + \frac{[\text{B}]}{K_B}\right)} . \quad (1.32)$$

The double-reciprocal relationship is:

$$\frac{1}{r} = \frac{1}{n} + \frac{K_A}{n[\text{A}]} \left(1 + \frac{[\text{B}]}{K_B}\right) \quad (1.33)$$

and the Scatchard equation:

$$\frac{r}{[\text{A}]} = \frac{n}{K_A \left(1 + \frac{[\text{B}]}{K_B}\right)} - \frac{r}{K_A \left(1 + \frac{[\text{B}]}{K_B}\right)} . \quad (1.34)$$

Compared with the general binding equation there are now two variable concentration terms, but as long as one of them (e.g. B) remains constant and only A is altered, the term within the brackets will also remain constant and the behavior corresponds essentially to the general binding equation with a hyperbolic curve (Fig. 1.5A). The only difference is that the value of K_A is increased by the value of the term in brackets. If, in a second test series, another concentration of B is taken (but remains constant during the test series), the resulting curve will again be modified by a change in the apparent value of K_A . In this manner a series of hyperbolic curves are obtained. All can be linearized in the double-reciprocal plot (Fig. 1.5B), the Scatchard plot (Fig. 1.5C) and the Hanes plot (Fig. 1.5D). The pattern of the lines is remarkable, with a common ordinate intercept in the double-reciprocal diagram, a joint abscissa intercept in the Scatchard plot and parallel lines in the Hanes plot. These patterns can be taken as indicative of a competition mechanism.

While the dissociation constant K_A for the first ligand can be obtained as already described in the absence of B, the constant for B, K_B , can be derived e.g. from the abscissa intercept $K_A(1 + [\text{A}]K_B)$ in the double-reciprocal diagram from a knowledge of K_A .

Further procedures for the analysis of competition data are described in Section 2.5.3.3. It must, however, be considered, that, unlike with enzyme kinetic studies, competition is not always unequivocal and can easily be mixed up with the non-competitive mechanism, as is described in the following section.

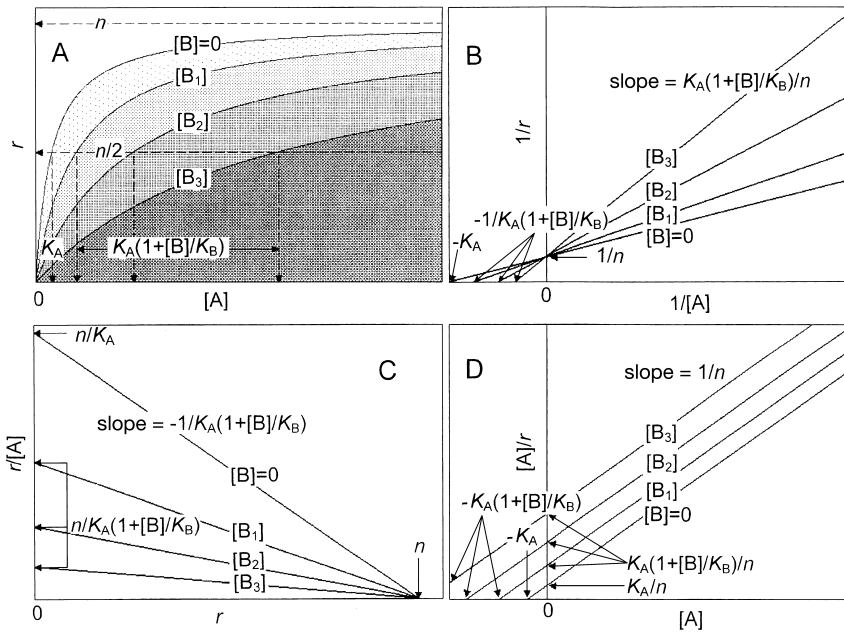
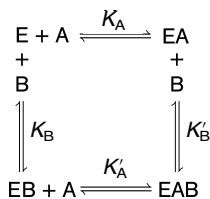


Fig. 1.5 Competition of a ligand for the same binding site. The concentration of ligand A is altered with ligand B at various, but constant amounts. (A) Direct plot, (B) double-reciprocal plot, (C) Scatchard plot, (D) Hanes plot.

1.3.4

Non-competitive Binding

A non-competitive binding mechanism exists if the second ligand induces the binding of the first one, but does not exclude its binding. While for competition it is assumed that both ligands bind to the same site, in the non-competitive mechanism both occupy different sites, which both influence one another, e.g. because of steric or electrostatic interactions.



Therefore the constants for binding to the free macromolecule, K_A and K_B , differ from those for the macromolecule occupied already with one ligand, K'_A and K'_B :

$$K'_A = \frac{[\text{EB}][\text{A}]}{[\text{EAB}]} \quad \text{and} \quad K'_B = \frac{[\text{EA}][\text{B}]}{[\text{EAB}]}, \quad (1.31 \text{ b})$$

and, considering also Eq. (1.31 a), they are linked

$$\frac{K_A}{K_B} = \frac{K'_A}{K'_B}. \quad (1.35)$$

The total amount of the macromolecule is:

$$[\text{E}]_0 = [\text{E}] + [\text{EA}] + [\text{EB}] + [\text{EAB}]$$

and the individual macromolecule forms can be eliminated by the constants defined in Eqs. (1.31 a, b):

$$[\text{E}]_0 = [\text{E}] + \frac{[\text{E}][\text{A}]}{K_A} + \frac{[\text{E}][\text{B}]}{K_B} + \frac{[\text{E}][\text{A}][\text{B}]}{K_A K'_B},$$

$$[\text{E}] = \frac{[\text{E}]_0}{1 + \frac{[\text{A}]}{K_A} + \frac{[\text{B}]}{K_B} + \frac{[\text{A}][\text{B}]}{K_A K'_B}}.$$

The portion of $[\text{A}]_{\text{bound}}$ is:

$$[\text{A}]_{\text{bound}} = [\text{EA}] + [\text{EAB}] = \frac{[\text{E}][\text{A}]}{K_A} + \frac{[\text{E}][\text{A}][\text{B}]}{K_A K'_B},$$

$$[\text{A}]_{\text{bound}} = \frac{\frac{[\text{E}]_0[\text{A}]}{K_A} \left(1 + \frac{[\text{B}]}{K'_B}\right)}{1 + \frac{[\text{A}]}{K_A} + \frac{[\text{B}]}{K_B} + \frac{[\text{A}][\text{B}]}{K_A K'_B}}.$$

The final equation for the non-competitive binding is obtained by replacing $[\text{A}]_{\text{bound}}$ by $r = [\text{A}]_{\text{bound}}/[\text{E}]_0$, assuming n binding sites and multiplying by K_A :

$$r = \frac{n[\text{A}] \left(1 + \frac{[\text{B}]}{K'_B}\right)}{K_A \left(1 + \frac{[\text{B}]}{K_B}\right) + [\text{A}] \left(1 + \frac{[\text{B}]}{K'_B}\right)}. \quad (1.36)$$

It is obvious that the equation will reduce to the normal binding equation if $K_B = K'_B$ (and, consequently $K_A = K'_A$), i.e. if there is no mutual interaction between both ligands. Transformation into the double-reciprocal form yields:

$$\frac{1}{r} = \frac{1}{n} + \frac{K_A \left(1 + \frac{[B]}{K_B}\right)}{n[A] \left(1 + \frac{[B]}{K'_B}\right)} \quad (1.37)$$

This will give a pattern of straight lines with a joint ordinate intercept, as shown in Fig. 1.5 B. Accordingly, the Scatchard plot

$$\frac{r}{[A]} = n \frac{\left(1 + \frac{[B]}{K'_B}\right)}{K_A \left(1 + \frac{[B]}{K_B}\right)} - r \frac{\left(1 + \frac{[B]}{K'_B}\right)}{K_A \left(1 + \frac{[B]}{K_B}\right)} \quad (1.38)$$

will yield a pattern of straight lines as shown in Fig. 1.5 C (the same situation holds also for the Hanes plot, Fig. 1.5 D). Obviously both competitive and non-competitive binding are indistinguishable by graphic analysis, and this is a serious source of misinterpretation, the more so, as both corresponding mechanisms in enzyme kinetics are readily distinguishable by graphic analysis (see Section 2.5.3.2). The reason for this discrepancy may not be immediately clear. In enzyme kinetics there is a similar situation with the partially competitive inhibition, which yields just the same pattern in linearized diagrams as the competitive mechanism (Section 2.5.3.7) and, in fact, non-competitive binding must be regarded as analogous to this and not to the non-competitive inhibition. This discrepancy arises because in non-competitive inhibition only the enzyme substrate complex [EA] is enzymatic active, while the complex with both substrate and inhibitor bound [EAI] is inactive. In contrast, with partially competitive inhibition both complexes are assumed to be equally active. This is just the situation in binding experiments, where the share of ligand A actually bound to the macromolecule will be determined by experiment which will not differentiate between [EA] and [EAB], regarding both as equally active. To avoid this misinterpretation, there exists a simple control. Plotting the slopes of the straight lines of the double-reciprocal diagrams against the concentration of the second ligand, B, must yield a straight line (with $-K_B$ as abscissa intercept) for competitive binding, but for non-competitive binding there is a deviation from linearity. Such secondary diagrams can also be derived from the Scatchard and the Hanes representations and are discussed in more detail in Section 2.5.3.2.

1.4

Macromolecules with Non-identical, Independent Binding Sites

Various enzymes, membrane receptors and other macromolecules possess different binding sites for the same ligand. They may be located at the same subunit, but more often they are an indication of the presence of non-identical subunits. An example is the bacterial tryptophan synthase, consisting of two types

of subunits (α, β), each binding indole as the intermediate of the enzyme reaction. Because the enzyme has the structure $\alpha_2\beta_2$, binding both to identical and non-identical sites occurs at the same time. Identical sites are called binding classes and one macromolecule can possess several (m) binding classes, each with several identical binding sites (n_1, n_2, n_3, \dots).

Obviously, a ligand binding to such a macromolecule will occupy the site with the highest affinity first, followed by occupation of the lower affinity sites, which require higher ligand concentrations. Assuming independent binding, each binding class will be saturated according to the general binding equation (Eq. (1.23)), so that the total binding process will be the sum of the individual saturation functions for each binding class:

$$r = \frac{n_1[A]}{K_{d1} + [A]} + \frac{n_2[A]}{K_{d2} + [A]} + \dots + \frac{n_m[A]}{K_{dm} + [A]} \quad (1.39)$$

K_{d1}, K_{d2} etc. are the dissociation constants of the individual binding classes. Each binding process follows a normal hyperbolic binding curve and the resulting function is a superposition of different hyperbolae (Fig. 1.6A). It shows a steep increase in the low concentration range of the ligand, where the high affinity site becomes occupied. At higher ligand concentrations, when this site becomes saturated, the low affinity sites will be occupied, resulting in a further, but smoother, rise of the curve. Although the curve does not have a pure hyperbolic shape, the deviation is difficult to recognize, especially with scattered data points; linearized plots are superior because they show characteristic deviations from linearity. Figures 1.6B–D show the individual (linear) curves for a high and a low affinity site and the resulting composed function in the double-reciprocal, the Scatchard and the Hanes diagram, respectively.

It is easier to create a composed function from the partial functions than to resolve the individual functions for the separate binding sites from a composed function obtained by experimental results. There are several unknown values to be determined, such as the number of binding classes involved, the number of identical sites per binding class and the values of the dissociation constants and it is impossible to get all the information from one curve. As can be seen from Fig. 1.6, the individual functions are not merely the asymptotes to the extreme ranges of the resulting curve, although it may be assumed that at very low and very high ligand concentrations the high and low affinity sites, respectively, will be occupied preferentially. The Scatchard plot can be analysed by using the graphic method of Rosenthal (1967) (Fig. 1.7). The resulting curve may be considered to be composed of two straight lines, the slopes of which are initially taken from both end parts of the resulting curve and are moved in a parallel manner so that the sum of their ordinate intercepts corresponds to the ordinate intercept of the resulting curve. Lines drawn through the coordinate origin meet the resulting curve at a point P. Its coordinates are the sums of the coordinates of the respective intersection points of the individual curves, as described for Fig. 1.7. For an appropriate evaluation a computer analysis is strongly recommended (Weder et al. 1976).

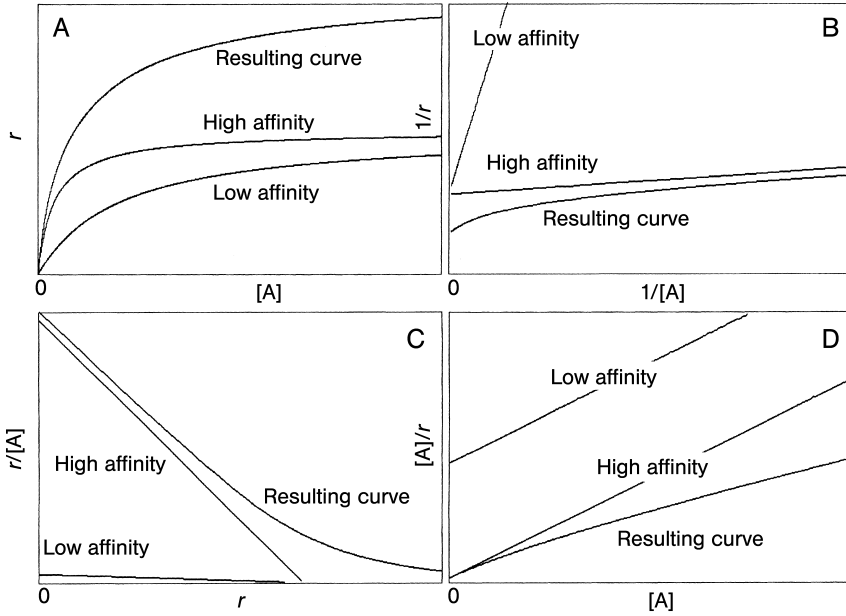


Fig. 1.6 Binding of a ligand to two binding classes of different affinity. The individual curves for the high and the low affinity site, and the resulting curve are shown. (A) Direct plotting, (B) double-reciprocal plot, (C) Scatchard plot, (D) Hanes plot.

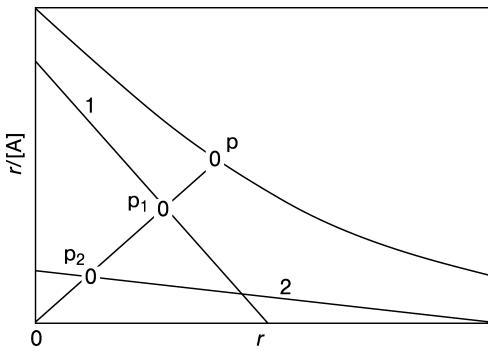


Fig. 1.7 Graphic analysis of a binding curve with two binding classes according to Rosenthal (1967). 1 and 2 are the lines of the separate binding classes. A straight line is drawn from the coordinate origin with the slope $1/[A]$, intersecting the individual lines

at P_1 and P_2 and the resulting curve at P . The sum of the coordinates $[A]_{\text{bound}}/([A]_{\text{bound}}/[A])$ of the individual intersection points must yield the coordinates of the resulting curve, otherwise, the position of the individual lines must be changed.

Nevertheless, the analysis of such binding curves has only indicative character. On the one hand there is no essential difference in the resulting curves with two or with more binding classes and, on the other hand, there are also other binding mechanisms, showing similar curves, like negative cooperativity and half-of-the-sites-reactivity (see Section 1.5.6) or isoenzymes. Determination of the number and identity of the subunits of the macromolecule by other methods, like molecular mass determination, should be undertaken in parallel.

1.5

Macromolecules with Identical, Interacting Binding Sites, Cooperativity

1.5.1

The Hill Equation

About one hundred years ago it was observed the binding of oxygen to hemoglobin does not follow a hyperbolic saturation function, according to the binding equation, but has a characteristic S- or sigmoidal shape (Bohr 1904). Remarkably, the closely related myoglobin behaves quite normally (Fig. 1.8). Since this time this atypical behavior of hemoglobin has challenged a large number of scientists to derive theoretical approaches and to develop fundamental techniques, like X-ray crystallography of proteins and methods for the detection of fast reactions. No other biological compound has inspired the development of biochemistry so much as hemoglobin. This atypical saturation behavior acquired even more interest when similar curves were found with enzymes occupying key positions in the metabolism. It became obvious that an important regulatory principle of the cell is hidden behind this phenomenon.

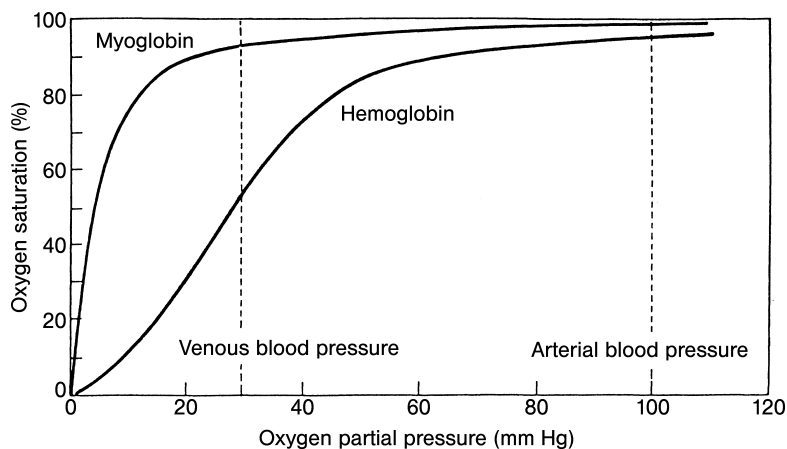


Fig. 1.8 Oxygen saturation curves for myoglobin and hemoglobin (according to M.F. Perutz, *Sci. Am.* 1978, 239(6), 68–86).

Archibald Vivian Hill undertook, in 1910, a first attempt to explain this atypical behavior. He suggested that not only one but several (n) oxygen molecules bind simultaneously to the hemoglobin molecule:



The dissociation constant according to the mass action law is defined as:

$$K_d = \frac{[E][A]^n}{[EA_n]} \quad (1.41)$$

and in analogy to Eq. (1.23) a binding equation can be derived for this mechanism, replacing $[A]$ by $[A]^n$:

$$r = \frac{n[A]^n}{K_d + [A]^n} . \quad (1.42)$$

This *Hill equation* indeed yields sigmoidal saturation curves. It was the intention of Hill to determine the number of oxygen molecules, n , actually binding to hemoglobin. This can be achieved by linearization of Eq. (1.42), replacing r by $\bar{Y}=r/n$ (the number 1 in the expression $\bar{Y}/(1-\bar{Y})$ has the significance of the saturation value):

$$\frac{\bar{Y}}{1-\bar{Y}} = \frac{[A]^n}{K_d} .$$

In a logarithmic form the power n enters into the slope:

$$\log \frac{\bar{Y}}{1-\bar{Y}} = n \cdot \log[A] - \log K_d \quad (1.43)$$

if the left term is plotted against $\log [A]$ (Fig. 1.9). Presupposing the validity of Eq. (1.43) a straight line should be expected and the number, n , of oxygen molecules bound to hemoglobin should be derived directly from the slope. However, the function obtained from the experimental data looks quite different. Instead of a linear dependence a characteristic three-phase behavior is revealed, starting from a slope of exactly 1 at low ligand concentrations, increasing to a maximum slope for the hemoglobin saturation curve of $n=2.8$, and thereafter decreasing again to 1 near saturation of $[A]$. Obviously, the function obtained deviates in two essential respects from the prediction of Eq. (1.43), the missing linearity and a slope lower than the expected value for the 4 subunits. It must be emphasized that this three-phase shape is not a special feature of hemoglobin but is observed with all enzymes showing sigmoidal saturation behavior. As can be easily seen, Eq. (1.43) becomes the normal binding Eq. (1.23) for $n=1$, and for this the Hill plot will indeed yield a straight line with a slope of exactly one.

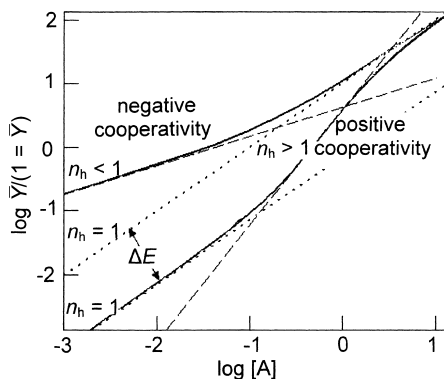


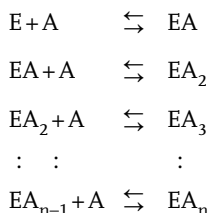
Fig. 1.9 Hill plot for positive and negative cooperativity. The dotted tangents to the curves in the lower and upper ligand ranges have a slope of 1, corresponding to normal hyperbolic binding. The Hill coefficient n_h is the slope of the dashed tangents to the maximum deviation.

Thus, the observed saturation behavior for sigmoidal curves appears to be a transition from two different, normal binding states at low and high ligand concentrations, respectively. This cannot be explained by the Hill equation and together with the wrong prediction of the number of binding sites n this equation may be regarded as useless. It is in fact not useful for describing sigmoidal saturation behavior, however, the diagram derived from this equation, still known as the *Hill plot*, proved to be a good graphic representation for any type of deviation from normal saturation behavior, as will be discussed later. It can also be used for the presentation of hyperbolic saturation curves, where both linearity and a slope of one is an indication of normal binding behavior. The abscissa intercept at half saturation, i.e. for $\log \bar{Y}/(1-\bar{Y}) = 0$, is K_d/n and becomes equal to K_d for $n=1$. Nevertheless, there is no real advantage over the other linearized diagrams to justify the circumstantial conversion of the experimental data.

1.5.2

The Adair Equation

Hill had no knowledge of the real structure of hemoglobin and did not realize that the number of binding sites was underestimated by applying his equation. It was 15 years later when G.S. Adair established that hemoglobin actually consists of four subunits and, thus, four oxygen molecules should bind. He derived an approach for the description of sigmoidal binding behavior, which, although some modifications have to be considered later, remains valid today in its fundamental aspects. He showed that the mechanism suggested by Hill is an oversimplification. If more than one ligand binds to a macromolecule, inevitably a consecutive binding process must be assumed. Even at high ligand concentrations binding will be initiated by occupation of one binding site by the first ligand, followed by binding of the second one, and so on, until all sites are occupied. This is formulated by the reaction sequence:



The sum of this reaction sequence:



is identical with Scheme (1.40) from which Hill derived his equation. In fact he ignored intermediate binding steps and allowed only simultaneous binding of all ligands. Binding of single ligands is strictly forbidden by this mechanism and it remains to be explained how a macromolecule will manage to avoid binding of individual ligands and allow only occupation of all sites at the same time. Comparable processes can be imagined for crystallization and polymerization reactions. Each chemist knows from his own experience that crystallization, even from pure, oversaturated solutions, can require days or weeks or may not occur at all. However, addition of seed crystals or even scratching at the glass wall will immediately provoke the formation of crystals in the whole solution. Similar processes are observed by the formation of fibers, like actin and myosin, from their subunits, where also the first aggregation step is strongly disfavored. For a macromolecule with several binding sites, it must be assumed that their affinity for the ligand is negligible, but just at the moment when one ligand binds, all sites acquire a high affinity state and thus the binding of one ligand entails instantaneous binding of all others. Actually, such exclusive binding is not very realistic and macromolecules, like haemoglobin, possessing more binding sites cannot reject the binding of a single ligand molecule. However, this first binding can strongly favor the binding of the following ligands. Such mechanisms, which assume that one ligand supports binding of others is called *cooperativity*. The Hill equation describes an extremely strong, not very probable, cooperativity, while the approach of Adair describes this phenomenon on a more realistic basis.

The derivation of the Adair equation has already been anticipated in Box 1.1 by the derivation of the general binding equation. The saturation function is defined as r , the ratio of the bound ligand $[A]_{\text{bound}}$ to the total enzyme $[E]_0$, both expressed by the different enzyme forms:

$$r = \frac{[A]_{\text{bound}}}{[E]_0} = \frac{[EA] + 2[EA_2] + 3[EA_3] + \dots + n[EA_n]}{[E] + [EA] + [EA_2] + [EA_3] + \dots + [EA_n]} \quad (1.44)$$

The intermediate enzyme forms are substituted by the macroscopic binding constants for the individual binding steps i .

$$K'_i = \frac{[\text{EA}_{i-1}][\text{A}]}{[\text{EA}_i]}.$$

In contrast to the general binding equation, the individual binding constants cannot be replaced by one single common constant and, therefore, the *Adair equation* reads:

$$\begin{aligned} r &= \frac{\frac{[\text{A}]}{K'} + \frac{2[\text{A}]^2}{K'_1 K'_2} + \frac{3[\text{A}]^3}{K'_1 K'_2 K'_3} + \dots + \frac{n[\text{A}]^n}{K'_1 K'_2 K'_3 \dots K'_n}}{1 + \frac{[\text{A}]}{K'_1} + \frac{[\text{A}]^2}{K'_1 K'_2} + \frac{[\text{A}]^3}{K'_1 K'_2 K'_3} + \dots + \frac{[\text{A}]^n}{K'_1 K'_2 K'_3 \dots K'_n}} \\ &= \frac{\sum_{i=1}^n \frac{i[\text{A}]^i}{\left(\prod_{j=1}^i K'_j\right)}}{1 + \sum_{i=1}^n \frac{[\text{A}]^i}{\prod_{j=1}^i K'_j}}. \end{aligned} \quad (1.45)$$

Since now every binding step gets its individual binding constant, the change in the affinity from the first to the following binding steps can easily be demonstrated. Increasing affinity can be realized by decreasing values for the binding constants $K'_1 > K'_2 > K'_3 \dots$. Under these conditions sigmoidal saturation curves are obtained and they show indeed the three-phase behavior in the Hill plot, as observed by applying real saturation data of hemoglobin with oxygen. Since the binding constants for each individual step cannot be obtained directly, they must be estimated and adapted until the theoretical curve fits the experimental data satisfactorily. The maximum steepness of the curve depends on the ratio of the individual constants, the more they differ, especially the higher the difference between the first and the last constant, the steeper the maximum slope. It can be seen that in any case the maximum slope ranges between 1 and n , the number of individual binding steps (usually identical with the number of binding sites, respectively, of identical subunits of the macromolecule). However, n cannot be surpassed by any combination of the constants. The maximum slope approaches n the higher the difference between the constants, while it approaches 1 the more the constants became equal to one another. From this consideration the value of 2.8 for oxygen binding to hemoglobin can be understood. The first oxygen raises the affinity for the following ones. If this rise is extremely strong, a value of 4 would be expected, corresponding to the four binding sites. In the case of only a moderate rise, a value between 1 and n will be obtained. So the maximum slope in the Hill plot is a measure of the cooperativity between the sites, a value near 1 meaning low cooperativity and a value near n high cooperativity. Different from the original assumption of Hill, the maximum slope indicates not the number of ligands bound or of binding sites on

the macromolecule, but is a measure of cooperativity, the knowledge of binding sites being presupposed. To differentiate from n , the number of identical binding sites, the maximum slope in the Hill plot is designated as n_h (or h). Although n_h does not indicate the actual number of binding sites, it gives a hint for their minimum number, since $1 < n_h < n$. For example, the value of $n_h = 2.8$ found for hemoglobin shows that this macromolecule must be composed of at least 3 identical subunits (n can only be an integer).

A comment should be made about the significance of n : it stands for the number of *identical* binding sites, identical meaning of equal affinity, characterized by equal dissociation constants. If they are different, deviations as discussed in Section 1.4 will be obtained. However, no presupposition is made as to whether these binding sites are localized on one single subunit or protein chain (e.g. generated by gene duplication) or on separated subunits, nor there is any presupposition as to whether these separate subunits must be identical or can be different. Obviously identical subunits possess identical binding sites, while even apparently identical sites localized at the same polypeptide chain can differ in their binding constants, due to dissimilar constraints of the protein molecule. Therefore, identical binding sites are usually assumed to be located on identical subunits and n stands both for identical binding sites and identical subunits, although this must be taken with caution. Regarding hemoglobin, it consists of non-identical ($\alpha_2\beta_2$) subunits, which is so far consistent with this consideration, as the binding constants can be taken as identical.

Although the Adair equation, in contrast to the Hill equation, is able to describe formally the experimental binding curves, it remains unsatisfactory as it is not based on a plausible binding mechanism. The Adair mechanism assumes that the binding steps, and not the binding sites of the macromolecule, differ in their affinity. In the absence of ligand all binding sites are regarded to be equal, and each binding step produces a defined change in the affinities of the still unoccupied binding sites. Consequently, the binding site of the macromolecule which becomes occupied last has to change its affinity n times, from K'_1 to K'_4 although it is not involved in the preceding binding steps. It is a theoretical mechanism, giving no explanation of how these affinity changes are achieved.

1.5.3

The Pauling Model

The first plausible description of cooperative phenomena was proposed in 1935 by Linus Pauling. He considered the macromolecule to consist of identical binding sites with an uniform binding constant K_d . He further assumed that the subunit occupied by a ligand confers a stabilizing effect on the unoccupied subunits enhancing their affinities, expressed by an interaction factor α . Considering the statistical factors described in Box 1.1, Eq. (2), the following constants can be ascribed to each individual binding step:

$$K'_{d1} = \frac{K_d}{4}; K'_{d2} = \frac{2K_d}{3a}; K'_{d3} = \frac{3K_d}{2a^2}; K'_{d4} = \frac{4K_d}{a^3}.$$

Entering these constants into the Adair equation, the following binding function results:

$$r = \frac{\frac{4[A]}{K_d} + \frac{12a[A]^2}{K_d^2} + \frac{12a^3[A]^3}{K_d^3} + \frac{4a^6[A]^4}{K_d^4}}{1 + \frac{4[A]}{K_d} + \frac{6a[A]^2}{K_d^2} + \frac{4a^3[A]^3}{K_d^3} + \frac{a^6[A]^4}{K_d^4}}. \quad (1.46)$$

Although this relationship is simpler than the Adair equation it gives an intuitive description of the sigmoidal binding mechanism.

1.5.4

Allosteric Enzymes

The first attempts to explain the sigmoidal binding behavior concentrated on the immediate effect of oxygen on hemoglobin. Subsequently, it became obvious that this atypical binding behavior is not restricted to hemoglobin alone, but is a feature of numerous key enzymes and that it concerns not only one single ligand like oxygen or an enzyme substrate, but it can be influenced by other ligands, called *effectors*. For distinction the direct effects of the single ligand are denoted as *homotropic effects*, while influences from effectors are called *heterotropic effects*. These influences can either be positive or negative and the respective effector acts, correspondingly, as *activator* or *inhibitor*. The effectors act not by direct interaction with the first ligand, e.g. by displacement from its binding site (competition), rather they occupy a spatially separate binding site. This is called an *allosteric center* from the Greek words *αλλος* for different and *στερεος* for rigid. Accordingly, enzymes showing these features are called *allosteric enzymes*. The separate allosteric center permits the regulation of the enzyme by metabolites, which are completely different from the physiological ligands of the enzyme, like substrates, cofactors or coenzymes. An important regulatory principle is the *feedback inhibition*. Metabolic pathways are frequently controlled by their end products, which inhibit the first step of the pathway, so that intermediates will not accumulate. The final product of the pathway is quite different from the substrate or product of the enzyme catalyzing the initial step and will be not recognized by its catalytic site. Therefore it binds to an allosteric center, from which it influences, e.g. by conformational change, the catalytic efficiency of the enzyme. It had been observed that allosteric effectors confer a characteristic influence on the sigmoidal saturation function of the substrate. Inhibitors, although reducing the catalytic efficiency, increase the homotropic effect by intensifying the sigmoidal shape of the saturation curve, while activators raise the catalytic efficiency by weakening the homotropic effect, converting the sigmoidal

shape of the saturation curve into a hyperbolic one. Theoretical approaches to explain cooperative effects with enzymes and related proteins must, therefore, also include heterotropic effects. It should be stressed, that *cooperativity*, i.e. increase of affinity of the same ligand upon consecutive binding and *allostery*, i.e. binding to spatially separated sites, are principally two independent phenomena, which may also occur separately in distinct enzymes. It is, however, an empirical observation that both features are usually combined in the same enzyme or protein system, since they both supplement one another and the regulatory power can be fully expressed only by combination of both phenomena. Therefore, it is justified to understand *allosteric enzymes* as a notation for enzymes revealing both cooperativity and allostery. Allostery is observed with various enzymes, but also with several non-enzyme proteins, like hemoglobin or the acetylcholine receptor and, therefore, in the following no differentiation is made between enzymes and proteins.

1.5.5

The Symmetry or Concerted Model

In 1965 Jacques Monod, Jeffries Wyman and Jean-Pierre Changeux presented the first comprehensive model for the description of allosteric enzymes in the publication *On the Nature of Allosteric Transition: A Plausible Model*. It became a guideline for the better understanding of regulatory mechanisms on enzymes. This *concerted or symmetry model* is based on certain presuppositions (see Fig. 1.10) which were deduced from observations made with hemoglobin and several allosteric enzymes:

1. An allosteric system is an oligomer composed of a defined number, n , of identical units (protomers). The protomer can either consist of a single subunit (polypeptide chain) or be composed of several non-identical subunits.
2. Protomers occupy equal positions in the macromolecule, there exists at least one symmetry axis.
3. The enzyme can accept at least two states of conformation termed T (*tense*) and R (*relaxed*), which differ in their energy potential. In the absence of ligand the transition from one into the other state occurs spontaneously, L being the equilibrium constant between both states:

$$L = \frac{[T]_0}{[R]_0} . \quad (1.47)$$

4. The molecular symmetry is preserved during the transition from one enzyme form to the other. At the same time all subunits of an enzyme molecule exist either in the T- or the R-state, intermediate forms with protomers in different conformations are excluded.
5. Both enzyme forms differ in their affinity for the ligand, T being the low affinity (or less active) and R the high affinity (or fully active) enzyme form, the ratio c of the dissociation constants for both forms is correspondingly:

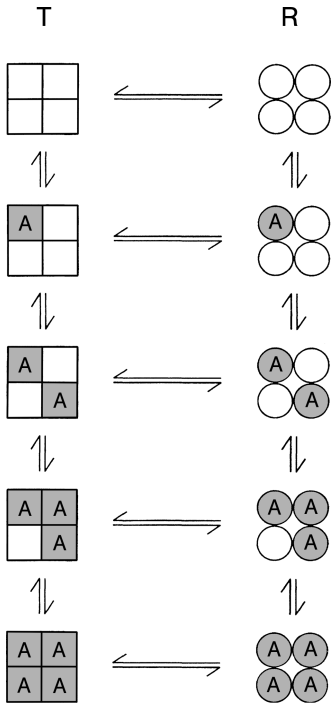
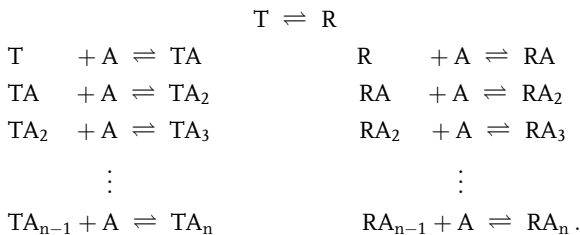


Fig. 1.10 Schematic representation of the conformational states and the fractional saturation of a tetramer macromolecule according to the symmetry model.

$$c = \frac{K_R}{K_T} < 1. \tag{1.48}$$

6. In the absence of ligand the equilibrium L is in favor of the low affinity form T , i.e. $L > 1$.

The binding of the ligand to the two enzyme forms is described by the equilibria:



The individual enzyme forms can be replaced by microscopic binding constants, which are assumed to be identical for all protomers in the same conformation:

$$\begin{aligned}
[\text{TA}] &= [\text{T}]n \frac{[\text{A}]}{K_{\text{T}}} & [\text{RA}] &= [\text{R}]n \frac{[\text{A}]}{K_{\text{R}}} \\
[\text{TA}]_2 &= [\text{TA}] \frac{(n-1)[\text{A}]}{2K_{\text{T}}} & [\text{RA}]_2 &= [\text{RA}] \frac{(n-1)[\text{A}]}{2K_{\text{R}}} \\
&\vdots & & \vdots \\
[\text{TA}]_n &= [\text{TA}_{n-1}] \frac{[\text{A}]}{nK_{\text{T}}} & [\text{RA}]_n &= [\text{RA}_{n-1}] \frac{[\text{A}]}{nK_{\text{R}}} .
\end{aligned}$$

From the fraction of the binding sites occupied by ligand

$$\bar{Y} = \frac{1}{n} \cdot \frac{([\text{TA}] + 2[\text{TA}_2] + \dots n[\text{TA}_n]) + ([\text{RA}] + 2[\text{RA}_2] + \dots n[\text{RA}_n])}{([\text{T}]_0 + [\text{TA}] + [\text{TA}_2] + \dots [\text{TA}_n]) + ([\text{R}]_0 + [\text{RA}] + [\text{RA}_2] + \dots [\text{RA}_n])} \quad (1.49)$$

the general saturation function for the symmetry model is obtained, replacing a for $[\text{A}]/K_{\text{R}}$, the ligand concentration, reduced by its dissociation constant:

$$\bar{Y} = \frac{Lca(1+ca)^{n-1} + a(1+a)^{n-1}}{L(1+ca)^n + (1+a)^n} . \quad (1.50)$$

Sigmoidal saturation curves are obtained when all three preconditions: $L > 1$, $c < 1$ and $n > 1$ are fulfilled simultaneously. If only one fails, c or n becoming 1 or L approaching to low values, Eq. (1.50) reduces to the general binding equation:

$$\bar{Y} = \frac{a}{1+a} = \frac{[\text{A}]}{K_{\text{R}} + [\text{A}]} . \quad (1.23)$$

Conversely, the cooperativity, or the sigmoidicity, of the saturation curve becomes more intense, the more these preconditions are fulfilled, i.e. the larger L and n and the smaller c . In the direct non-linear plot (Fig. 1.11 A) such changes are less detectable, while the linear plots show characteristic deviations from a straight line. In the double-reciprocal plot (Fig. 1.11 B) the curve deviates towards the upper right, in the Hanes plot (Fig. 1.11 D) to the upper left, and in the Scatchard plot (Fig. 1.11 C) a maximum is passed. Further information about the cooperative systems can be obtained from the Hill plot (Fig. 1.9). As already mentioned, the curve progresses from a straight line with a slope of 1 at low ligand concentrations through a steeper section in the medium saturation range and returns to a straight line with a slope of 1 in the saturation range. Both sections with the slope of 1 represent simple binding characteristics, to the T-state in the very low and the R-state in the high saturation range. The distance between the two straight lines is an indication of the energy difference between the R- and T-states. The cooperative effect is greatest in the steepest area, where the system switches from the low affinity T-state to the high affinity R-state. The maximum slope is the Hill coefficient (n_{H}) indicating the strength of cooperativity (see below).

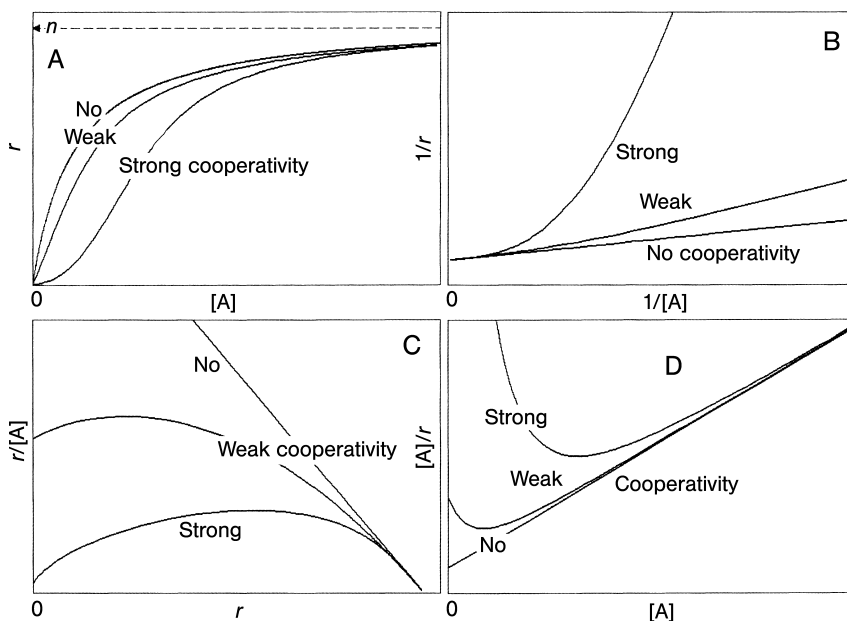


Fig. 1.11 Binding curves of cooperative systems according to the symmetry model in different representations. (A) Direct plot, (B) double-reciprocal plot, (C) Scatchard plot, (D) Hanes plot. No cooperativity: $L=c=1$; weak cooperativity: $L=5$, $c=0.1$; strong cooperativity: $L=100$, $c=0.01$.

The cooperative effect can be illustrated by considering that the first binding ligand will find only a few molecules in the high affinity R-state out of a surplus of non-binding molecules in the T-state. Binding will stabilize the R-state and withdraw it from the equilibrium. To restore the original equilibrium a molecule from the T-state will be converted into the R-state. Thus, for the following ligand, four additional binding sites (assuming $n=4$ for this example) are accessible. The number of accessible binding sites thus increases faster than the ligand concentration causing a disproportionate increase in binding or activity. This process will proceed until the pool of molecules in the T-state is depleted and the whole macromolecule population is shifted to the R-form. Then cooperative binding changes to normal binding and the slope in the Hill plot reduces to 1.

The relative size of the Hill coefficient between the limits $1 < n_h < n$ is determined by the values of L and c : the better the conditions $L \gg 1$ and $c \ll 1$ are fulfilled, the more n_h will approach the number of protomers n . In no case, however, can n be surpassed by n_h . Conversely, n_h cannot fall below 1 with any combination of L and c . The Hill coefficient thus proves to be a measure of the strength of cooperativity. The more it approaches the number of protomers, the more pronounced the cooperativity becomes. In the extreme case of $n_h = n$ the mechanism defined by the Hill equation (Eq. (1.42)) applies. In its strict definition the Hill coefficient indicates

Table 1.1 Relationship between the number of protomers n and the Hill coefficient n_h with heme proteins from different organisms (after Wyman 1967)

Protein	Source	n	n_h
Myoglobin	Mammalian	1	1
Myoglobin	Molluscs	2	1.5
Hemoglobin	Mammalian	4	2.8
Hemocyanin	Lobster	24	4
Chlorocruorin	<i>Spirographis</i>	~80	5
Erythrocrurorin	<i>Arenicola</i>	>100	6

the reaction order with respect to the varied ligand. According to Eq. (1.40), n should only be an integer but since the mechanism depends on the strength of subunit–subunit interactions a fractional reaction order can also exist. The highest possible reaction order, i.e. maximal cooperativity, is achieved when all binding sites become simultaneously occupied. Therefore, the Hill coefficient is not a direct measure of the number of binding sites (or protomers), but ranges between 1 and n (as long as no other mechanism is responsible for the sigmoidal curve). There exists, however, no direct proportionality between n_h and n . An increase in n is not paralleled by a similar increase in n_h , even for identical values of L and n . In Table 1.1 oxygen-binding proteins from different organisms are compared with their number of protomers and the observed Hill coefficients. While n increases from 1 to 100 the Hill coefficient only rises to 6. This follows also from theoretical calculations.

Heterotopic effectors influence the equilibrium of R- and T-states by binding to allosteric centers. Activators act in the same manner as the cooperative ligand. They bind preferentially to the R-form and shift the equilibrium in this direction. L becomes diminished in the presence of the activator, the cooperativity will be attenuated and the Hill coefficient decreases. Consequently, in the presence of the activator the macromolecule will persist essentially in the R-state, so that the original cooperative ligand will find only the active R-state and bind to this in a quite normal, non-cooperative manner. Conversely, the inhibitor binds to and stabilises the T-form, increasing L and, subsequently, n_h , intensifying the cooperativity. Larger amounts of ligand are now required to shift the equilibrium towards the R-form, revealing an inhibitory effect.

The influence of effectors can be considered in Eq. (1.50) by modifying the equilibrium constant from L to L' . The meaning of L' is:

$$L' = L \left(\frac{1 + d\beta}{1 + \beta} \right)^n \cdot \left(\frac{1 + e\gamma}{1 + \gamma} \right)^n \quad (1.51)$$

β and γ are the concentrations of inhibitor, or activator, reduced by their respective binding constants K_{Ri} and K_{Ra} to the R-form; $d = K_{Ri}/K_{Ti} > 1$ and $e = K_{Ra}/K_{Ta} < 1$ are the ratios of the binding constants for the R- and T-states of inhibitor and activator, respectively.

1.5.6

The Sequential Model and Negative Cooperativity

One year after the postulation of the concerted model D. E. Koshland, G. Nemethy and D. Filmer (1966) presented an alternative model for allosteric enzymes which describes the cooperative phenomena and heterotopic effects equally well. The general prerequisites are comparable, the macromolecule is assumed to be composed of several identical subunits and exists in at least two conformations, differing in their affinity. The low affinity or inactive T-state (for uniformity the terms from the concerted model are also applied here) prevails in the absence of ligand, the high affinity or fully active R-state in the presence of ligand. K_t is the equilibrium constant of both enzyme forms in the absence of ligand:

$$K_t = \frac{[T]}{[R]} \gg 1. \quad (1.52)$$

There exist two substantial differences from the concerted model. Before postulating the sequential model Koshland developed the *induced-fit hypothesis*. It replaced the previous *lock-and-key model* of Emil Fischer (1894), which assumed that substrate specificity of enzymes is based on preformed rigid binding regions, into which only the proper substrate molecule can lock like a key. In comparison with this theory the induced-fit hypothesis predicted that the binding site would be created interactively by enzyme and substrate. Only the actual substrate is able to induce this adaptation. This hypothesis is a fundamental prerequisite for the sequential model. Unlike the concerted model, where the ligand is not actively involved in the shift from the T- to the R-state but only selects the form with higher affinity, the sequential model assumes that conformation transition is induced by the binding of the ligand. As a second difference from the concerted model a sequential transition is assumed, only subunits to which the ligand binds change into the R-form, all others remain in the T-state. The transition occurs stepwise in parallel with the saturation of the enzyme (Fig. 1.12).

Cooperativity originates from the interaction between the subunits. The intensity of the interaction depends on the conformational state of the neighboring subunits and is defined by interaction constants. They indicate the ratio of interacting (e.g. TT) to non-interacting subunits (T, T). As these are relative factors, the constant K_{TT} for the TT-interactions is defined as 1:

$$K_{TT} = \frac{[T][T][TT]}{[TT][T][T]} = 1 \quad (1.53)$$

$$K_{RT} = \frac{[T][R][RT]}{[RT][T][T]} = \frac{[R][TT]}{[RT][T]} \quad (1.54)$$

$$K_{RR} = \frac{[R][R][RT]}{[RR][T][T]}. \quad (1.55)$$

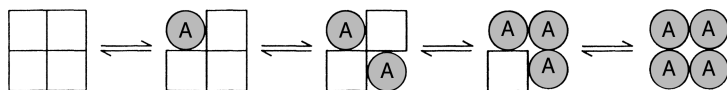


Fig. 1.12 Schematic representation of the conformation states and the fractional saturation of a tetrameric macromolecule according to the sequential model.

The interactions between the subunits can either be stabilizing (K_{RT} and $K_{RR} < 1$) or destabilizing (K_{RT} and $K_{RR} > 1$).

The saturation function for the sequential model is derived from the general form of the Adair equation (Eq. (1.45)):

$$\bar{Y} = \frac{1}{n} \cdot \frac{\frac{[A]}{\theta_1} + \frac{2[A]^2}{\theta_2} + \frac{3[A]^3}{\theta_3} + \dots + \frac{n[A]^n}{\theta_n}}{\theta_0 + \frac{[A]}{\theta_1} + \frac{[A]^2}{\theta_2} + \frac{[A]^3}{\theta_3} + \dots + \frac{[A]^n}{\theta_n}} \quad (1.56)$$

The terms θ_0 , θ_1 etc. include all constants relevant for the respective binding step: the constant K_R for binding of the ligand to the R-state (binding to the lower affinity T-state is neglected), the constant K_t for the equilibrium between the two macromolecule forms, and the substrate concentration $[A]$ considered in the equation with the power of the respective binding step i . The possible interactions between subunits determine the type of interaction constants to be considered for each binding step. This is demonstrated in Table 1.2 for the case of a macromolecule consisting of three identical subunits in a linear arrangement. Although such an arrangement is highly improbable, it is taken as a simple model to demonstrate the derivation of a rate equation in the sequential model. By inserting the θ links into Eq. (1.56) the following equation results:

$$\bar{Y} = \frac{1}{3} \cdot \frac{\frac{[A]}{(K_{RT}^2 + 2K_{RT})K_R K_t} + \frac{2[A]^2}{(K_{RT}^2 + 2K_{RT}K_{RR})K_R^2 K_t^2} + \frac{3[A]^3}{2K_{RR}^2 K_R^3 K_t^3}}{1 + \frac{[A]}{(K_{RT}^2 + 2K_{RT})K_R K_t} + \frac{[A]^2}{(K_{RT}^2 + 2K_{RT}K_{RR})K_R^2 K_t^2} + \frac{[A]^3}{2K_{RR}^2 K_R^3 K_t^3}} \quad (1.57)$$

Because this model rests on the respective types of interactions each aggregation state and each arrangement of subunits needs its own derivation and the above equation is valid only for the trimeric arrangement. In Fig. 1.13 some aggregation states and subunit arrangements are depicted. Obviously the number of possible arrangements increases with the number of subunits, e.g. for a tetramer there exist three symmetric orientations, linear, square and tetrahedral. This complicates the treatment of the model. Whereas for the concerted model one single equation can be applied for any oligomer, for the sequential model not only the number, but also the respective arrangement of subunits must be known. Furthermore, it must be considered that with higher aggregates different interactions can occur, even between identical subunits. For example a hexamer composed of two trimers will

Table 1.2 Conformation states and definitions of the θ -values for a trimeric macromolecule with the subunits in a linear arrangement according to the sequential model

Enzyme conformation	Interaction constants	θ values
<i>Free enzyme</i>		
TTT	$K_{TT}K_{TT}=1$	$\theta_0=1$
<i>1st Binding step</i>		
TRT	$K_{RT}K_{RT} = K_{RT}^2$	$\theta_1 = (K_{RT}^2 + 2K_{RT})K_R K_t$
TTR+RTT	$K_{TT}K_{RT} + K_{RT}K_{TT} = 2K_{RT}$	
<i>2nd Binding step</i>		
RTR	$K_{RT}K_{RT} = K_{RT}^2$	$\theta_2 = (K_{RT}^2 + 2K_{RT}K_{RR})K_R^2 K_t^2$
RRT+TRR	$K_{RT}K_{RR} + K_{RR}K_{RT} = 2K_{RT}K_{RR}$	
<i>3rd Binding step</i>		
RRR	$K_{RR}K_{RR} = K_{RR}^2$	$\theta_3 = K_{RR}^2 K_R^3 K_t^3$

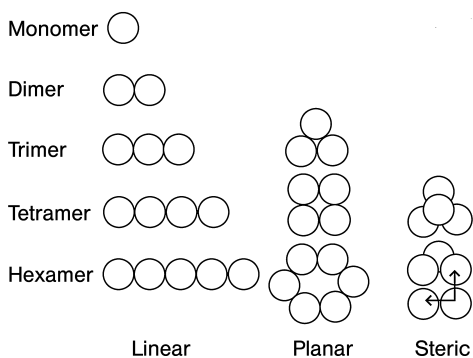


Fig. 1.13 Possible arrangements of subunits of differently aggregated macromolecules. Different horizontal and vertical subunit contacts for the hexamer are indicated by arrows at the bottom right.

possess other interactions within the trimer structure (Fig. 1.13, horizontal arrow), than those between the contact regions of the two trimers (Fig. 1.13, vertical arrow). For each type of contact site individual interaction constants must be defined.

Such complications render the application of the model more difficult and also the interaction constants are usually not accessible and must be estimated. However, the significance of both models rests not in their relative ease of treatment, but on their ability to gain a better understanding of regulatory mechanisms for which both models provide a clear conceptual basis. More information on the existence of one of these models for a distinct enzyme or protein requires detailed structural and conformational studies. One indication for the prevalence of one of the two models can be the relative position of the cooperative area (i.e. the maximum slope in the Hill plot) within the saturation function. In the sequential model it coincides exactly with the half-saturation range, in the concerted model this area shifts with rising n to the lower saturation range.

Heterotropic effects can be explained in the sequential model in a similar manner as in the concerted model. Allosteric activators reduce the cooperative effect by inducing the transition from the inactive to the active state like the cooperative ligand or substrate, while allosteric inhibitors strengthen the cooperative effect by stabilizing the T-state.

A special feature of the sequential model is the fact that interactions need not be stabilizing, but may also be destabilizing if K_{TR} and K_{RR} are larger than K_{TT} . The deviation from the normal hyperbolic saturation function is reversed to sigmoidal curves, rather it resembles that of non-identical independent binding centers (see Section 1.4), and in the linearized plots corresponding deviations result (see Fig. 1.6). In the Hill plot, instead of a maximum slope higher than 1 in the cooperative range, a minimum slope less than 1 is obtained. This anti-cooperative behavior, which is in contrast to normal cooperativity (also termed *positive cooperativity*) is defined as *negative cooperativity*. It is observed in several enzymes. The first example was the binding of NAD to glyceraldehyde-3-phosphate dehydrogenase and served as evidence for the validity of the sequential model (Convay and Koshland 1968).

In a strict sense many examples of negative cooperativity actually obey the mechanism of *half-of-the-sites reactivity*. The first ligand occupies one site of the macromolecule and interferes with the binding to the second site by steric or electrostatic interactions or by covalent reactions, like phosphorylation, so that occupation of the second, originally identical, site becomes aggravated. Thus only half of the original binding sites are saturated, the other half remains unsaturated or requires very high ligand concentrations for saturation. Although the binding behavior and the respective graphical representations are very similar it is not a genuine negative cooperativity mediated by interaction of subunits. Half-of-the-sites reactivity was observed e.g. with alcohol dehydrogenase, malate dehydrogenase and alkaline phosphatase (Levitzki and Koshland 1976).

Obviously, evaluation of binding curves which deviate from normal behavior in a sense like negative cooperativity is difficult because of several alternative explanations, such as half-of-the-sites reactivity, non-identical binding centers, different enzyme forms or isoenzymes. Additional information, especially from structural studies, is required to differentiate, with regard to negative cooperativity and half-of-the-sites reactivity, between identical subunits and non-identical subunits. A negative cooperative mechanism has been reported for many macromolecules like glyceraldehyde-3-phosphate dehydrogenase, CTP-synthetase, desoxythymidine kinase, receptors and binding of tRNA to ribosomes. The physiological advantage of negative cooperativity may be the greater insensitivity to fluctuations in the concentration of metabolites, like substrates or effectors. Due to the high affinity of the first binding step these systems are already very active and able to maintain a basic turnover at low substrate levels. A larger increase in the substrate concentrations causes only a small further activity increase, but the system is able to follow substrate variations over a wide range in a damped mode without reaching early saturation.

1.5.7

Analysis of Cooperativity

Observation of atypical, i.e. sigmoidal saturation behavior with a distinct system is a first indication for the prevalence of cooperativity. Since the main mechanisms are based on the change in binding constants (*K*-systems), for analysis binding measurements are recommended. Since changes in the substrate affinity influences the enzyme reaction via the K_m -value, measurements of enzyme activity, which are easier to perform, can also yield sigmoidal dependences. Alternatively, the two enzyme conformations can differ in their catalytic activity instead of in their affinity (*V*-systems). A combination of both binding and kinetic measurements will give valuable additional information. This holds also for the action of the effectors, which can also be studied by both techniques. For the analysis of sigmoidal curves, linearized plots are preferable to direct, non-linear representations, as deviations from the linear progression are easily detectable (Fig. 1.11). These curves can be linearized by entering $[A]^{n_h}$ instead of $[A]$, where the Hill coefficient n_h (indicating the reaction order for $[A]$) and not the number of binding sites n must be used. To establish a cooperative mechanism a larger number of measurements is required than for hyperbolic systems and a broader concentration range of the ligand has to be covered.

Deviations from normal behavior may, however, have other reasons. Sigmoidal saturation curves can be observed in multiple substrate reactions, but artificial effects can also cause such curves. Enzymes are often unstable in dilute solutions and when a test series is performed from high to low substrate concentrations, the rates for the latter experiments may slow down because of this effect. A further source of error is the underestimation of initial velocities in the lower substrate range, especially with high amounts of enzyme, as will be discussed in Section 2.3.2. With high enzyme concentrations the assumption $[A]_0 = [A]$ is also no longer valid, which can also lead to misinterpretation.

As already mentioned an estimation of the strength of cooperativity is the relationship between the Hill coefficient and the number of binding sites n , with positive cooperativity n_h ranging between 1 and n , and with negative cooperativity tending to be below 1. In the Hill plot sigmoidal saturation curves usually show a three phase course, from a straight line with $n_h = 1$ across a steeper region with a maximum Hill coefficient to again a straight line with $n_h = 1$. Both straight lines represent the two enzyme states and the distance between both asymptotes multiplied by $RT\sqrt{2}$ yields the difference between the free energies for the binding interaction of the first and the last ligand (Fig. 1.9). The respective dissociation constants for both states can be estimated from the ligand concentration at the position of half saturation: $\log \{\bar{Y}/(1 - \bar{Y})\} = 0$ for $\bar{Y} = 0.5$. Since the cooperative range is the transition area between both states, and this cooperative range is usually at half saturation of the system, no defined dissociation constant can be obtained. Nevertheless, as for a given system half saturation is always at a distinct ligand concentration, a half saturation constant is defined also for cooperative systems, which is, in contrast to real dissociation constants, termed $S_{0.5}$.

Sometimes the R_s -value is taken as a measure of cooperativity. It is defined as the ratio of ligand concentration at 90% and 10% saturation, for a normal hyperbolic saturation curve the R_s -value is always 81. With positive cooperativity, the curve becomes steeper and the R_s -value decreases with the strength of cooperativity, while it increases with negative cooperativity (Table 1.3). The Hill coefficient and the R_s -value are not directly related. The Hill coefficient records cooperativity at a certain point, i.e. at maximum deviation, while the R_s -value covers a wider ligand range, but the connection to the number of protomers is lost. The estimation of the R_s -value is depicted in the semi-logarithmic diagram in Fig. 1.14, which is especially suited for the plotting of broad ligand concentration ranges applied with cooperative systems. Because in this plot normal binding curves also reveal a sigmoidal shape, a distinction can only be made by the steepness of the curve. The abscissa value of the turning point of the curve at half-saturation indicates the K_d -value in the case of normal binding behavior, or the $S_{0,5}$ -value for cooperative systems.

Table 1.3 Comparison of the Hill coefficient n_h and the R_s -value (Taketa and Pogell 1965)

n_h	R_s
0.5	6570
1.0	81
2.0	9
4.0	3

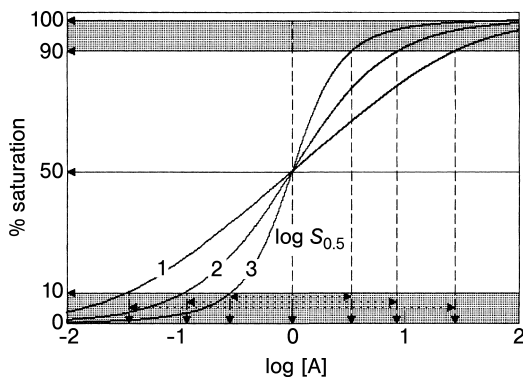


Fig. 1.14 Semi-logarithmic plot of saturation curves for the determination of the R_s -value from the ratio of ligand concentration at 90% and 10% saturation for 1) negative cooperative, 2) normal and 3) positive cooperative behavior. The ligand concentration at half-saturation (K_d - or $S_{0,5}$ -value) is assumed to be 1.

1.5.8

Physiological Aspects of Cooperativity

Cooperativity is one of the most important regulatory principles in the metabolism and is found, besides hemoglobin, in many key enzymes of metabolic pathways, in membrane-bound enzymes where it is influenced by membrane fluidity, in transport systems and ATPases, in receptor–ligand binding (e.g. the estrogen receptor), in acetylcholine esterase involved in synaptic transfer, and in thrombine activity. The advantage of (positive) cooperative saturation behavior rests in the over-proportional reaction of the system upon ligand fluctuations and in the allosteric regulation frequently connected with the cooperative effect. Allosteric regulation may also occur with normal binding systems without any cooperativity, when an effector binds to a separated site, which influences the active site. However, a normal system is not able to react in such a sensitive manner as a cooperative system. Due to the steep increase in the sigmoidal saturation curve in the middle saturation range that usually correlates with the physiological range of ligand variation (Fig. 1.15), a slight concentration shift causes a large activity change. The action of effectors is not only confined to inhibition or activation, they can also render the system less sensitive to substrate variations. The activator elevates the system to full activity, the inhibitor brings it down to a minimal level.

The question may be raised, which of the two models is preferred in nature or do alternative mechanisms, not covered by these models, exist. Actually the essential predictions of these models have proved correct, e.g. identical subunits, distinct conformations differing in their affinity, and allosteric regulatory sites. In the following, thoroughly investigated examples of allosteric macromolecules will be presented and it will be shown that aspects of both models can be found, sometimes even in the same system. As shown in Fig. 1.16, both models occupy extreme positions among all conceivable combinations of conformation transitions. The concerted model permits only the uniform conformations bordered in the outer bands, the sequential model only the diagonal states of direct linkage of ligand binding and conformation transition. So both models

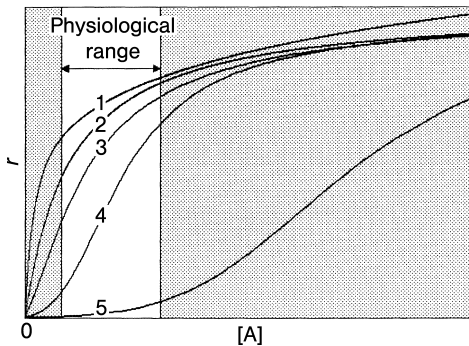


Fig. 1.15 Regulatory significance of allosteric enzymes. The physiological ligand range is highlighted 1) Negative cooperativity, 2) normal binding, 3) positive cooperativity with activator, 4) without effector and 5) with inhibitor.

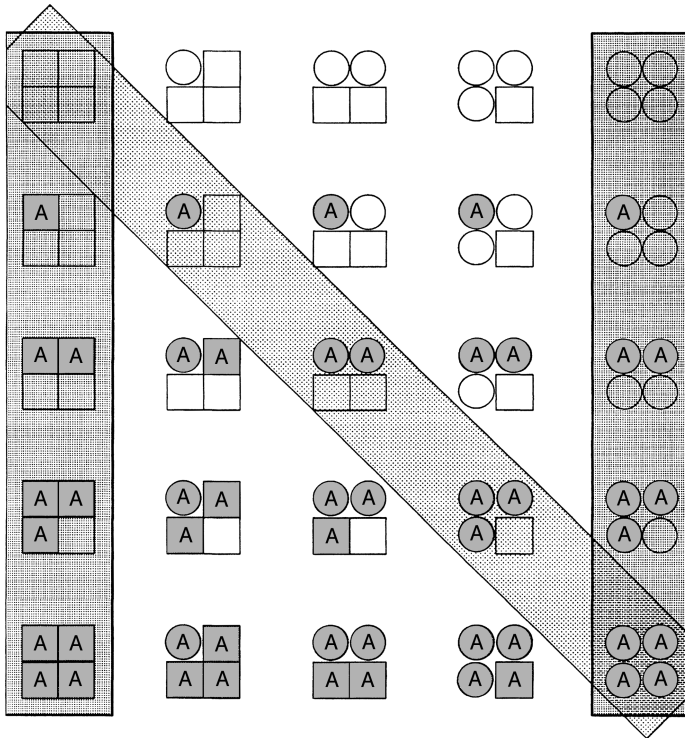


Fig. 1.16 Possible conformational and binding states of a tetrameric macromolecule. The lower affinity T-forms are presented as squares, the high affinity R-forms as circles. The vertical bars at the left and right enclose the states permitted in the concerted model, the diagonal bar the states assumed in the sequential model.

comprise already all plausible combinations. States not considered by them may also be included, but it is obvious that high cooperativity can only be obtained from the extreme positions. Therefore, an alternative model cannot be created without contributing additional aspects.

A test criterion for both models is their requirement of identical subunits. Cooperativity cannot be described with a monomeric macromolecule (with the exception that a macromolecule existing as a monomer in one state will aggregate to form the other state). Ribonuclease was the first example of an exclusively monomeric enzyme with sigmoidal saturation behavior. The cooperativity cannot be caused by interaction of subunits and thus is also not explained by the two models discussed so far. This phenomenon can, however, be explained by the ratio of the time dependences of the transition between the two states and the catalytic conversion of substrate to product, if the catalytic step is faster than the conformational transition. In contrast to both allosteric models, which are

based on equilibria, here kinetic, non-equilibria states are considered. This is, therefore, termed *kinetic cooperativity* and can only be detected in the presence of the catalytic turnover, i.e. by observing product formation, while binding measurements will yield normal saturation behavior. A plausible model, the *slow transition model*, has been derived, which will be described in Section 2.8.2.

In the last decades more detailed information about allosteric systems has been gathered which refines the picture of this class of proteins and enzymes. The existence of separate centers for regulation and for action has been widely established, the average distance between the centers being 3.0–4.0 nm. A more unexpected feature is the fact that binding sites for substrates as well as regulatory sites can be located at subunit interfaces rather than at a distinct subunit. In muscle nicotine receptor the binding sites for acetylcholine are located at subunit boundaries.

It also turns out that the assumption of only two states is a simplification valid possibly only for distinct systems, while different sub-conformations are assumed in other cases, e.g. that distinct subunits in one (the T-) state can adopt conformations leading to the other (R-) state.

A further extension of the allosteric models is to membrane inserted structures, like membrane receptors and transmembrane ion channels, where the regulatory sites, to which (e.g.) the neurotransmitter binds, is at one side (synaptic side) of the membrane, with the active center on the opposite site of the membrane, so that the interaction between the two different sites is mediated by a transmembrane allosteric transition. Equilibrium (in the absence of the ligand) prevails between a silent resting state and an active (e.g. open channel) state, agonists stabilizing the active and antagonists the silent state. A consequence of transmembrane polarity given by the two opposite sites is the existence of only one symmetry axis, perpendicular to the membrane plane.

1.5.9

Examples of Allosteric Enzymes

1.5.9.1 Hemoglobin

Although not an enzyme, hemoglobin has given invaluable impetus for numerous theoretical and experimental approaches, like the cooperative models, or the advancement of fast kinetic techniques and X-ray structural analysis. The comparison of the sigmoidal characteristics for oxygen binding to tetrameric hemoglobin with the hyperbolic saturation behavior of the closely related monomer myoglobin demonstrates clearly the significance of the interaction of subunits for cooperativity. As an apparent contradiction to the postulates of the cooperative models, hemoglobin consists of two pairs of non-identical subunits $\alpha_2\beta_2$ and should rather be regarded as a dimer consisting of two protomers. Accordingly, the Hill coefficient should not be greater than a value of 2, but a value of nearly 3 is actually found. The α - and β -subunits, however, possess not only a comparable structure, but also their affinities to oxygen are similar and thus they may be regarded as identical. X-ray crystallographic studies by Max Perutz

(1970, 1990) permit a detailed insight into the allosteric and cooperative machinery of hemoglobin. In the absence of oxygen (*desoxyhemoglobin*) hemoglobin is in a T-state of low affinity that is stabilized against the R-state of the oxygen-rich *oxyhemoglobin* by eight additional salt bridges between the subunits. Cleavage by carboxypeptidase of the C-terminal His and Tyr residues, which are involved in salt bridges, results in a non-cooperative form with high affinity for oxygen.

The divalent iron ion is complex-bound to the haem cofactor, coordinated by four porphyrine nitrogen atoms. In desoxyhemoglobin the iron exists in a high-spin state, emerging 0.06 nm out of the plane of the porphyrine ring, stabilized by a histidine residue on the fifth coordination site. The oxygen molecule binds to the sixth coordination site. This causes the iron to adopt the low-spin state and to move into the plane of the porphyrine ring, dragging along the histidine and inducing a conformational change in the R-state by cleaving the eight salt bridges between the subunits. The bound oxygen molecule stabilizes the R-state.

The significance of the sigmoidal saturation behavior for the regulation of the oxygen binding is demonstrated by its dependence on the concentration of protons (*Bohr effect*). The protons released from hydrogen carbonate in the blood capillaries bind to the terminal amino acids of hemoglobin and stabilize the T-state. The sigmoidicity of the saturation function becomes more pronounced, the binding capacity decreases and oxygen is released into the tissue. In contrast, higher oxygen binding caused by the elevated oxygen pressure in the lung releases protons from the hemoglobin, pH is lowered and the sigmoidicity decreases, induced by the stabilized R-state. The low pH in turn induces the release of CO₂ from hydrogen carbonate in the lung. 2,3-Bisphosphoglycerate stabilizes the T-state by connecting the β -subunits and decreases the oxygen binding capacity.

Recent investigations revealed aspects, which are not in accord with the mere symmetry model and require an extension. By encapsulation of hemoglobin in silica gel the T- and the R-states could be stabilized and it could be shown that subunits in the T-state can adopt R-like properties which is not merely consistent with the concerted model (Viappiani et al. 2004). Obviously heterotopic effects causing tertiary structural changes play a much greater role in determining the function of hemoglobin than do the homotopic T and R transitions in the quaternary structure (Yonetani et al. 2002).

1.5.9.2 Aspartate Transcarbamoylase

This enzyme from *Escherichia coli* clearly demonstrates the spatial separation of catalytic and regulatory centers on distinct polypeptide chains. The native enzyme molecule consists of six catalytic subunits (C, $M_r=33\,000$), joined in two trimers, and six regulatory subunits (R, $M_r=17\,000$) that form three dimers, resulting in a (C₃)₂(R₂)₃ structure. Catalytic and regulatory centers are 6 nm apart. The allosteric activator ATP and the inhibitor CTP both bind to the same region at the R-subunit. CTP stabilises the T-state and enhances the sigmoidal character of the substrate saturation function. ATP binds preferentially to the R-form

and weakens the cooperativity of the substrate aspartate which also binds preferentially to the R-form. At the transition from the T- to the R-state the two catalytic trimers move apart by 1.1 nm and rotate by 12° in relation to each other, while the regulatory dimers rotate by 15° around the two-fold molecule axis. Because of this transition several amino acid residues important for the binding of aspartate move towards the active center and increase the affinity for the substrate. The removal of the regulatory subunits results in the loss of cooperativity and the regulation by ATP and CTP, while the catalytic activity is retained. With this enzyme it was also possible to demonstrate the concerted transition from the T-state to the R-state according to the symmetry model. The occupation of half of all binding sites by the transition state analog *N*-phosphoacetyl-L-aspartate (PALA) is sufficient to transfer the entire enzyme molecule into the R-state.

Aspartate transcarbamoylase is a good example of end-product inhibition. The enzyme catalyzes the initial reaction of the pyrimidine nucleotide biosynthesis pathway and is inhibited by CTP, the end-product of the pathway. The activator ATP is the end-product of the purine biosynthesis pathway. As for the nucleic acid biosynthesis, both nucleotides are required in an equal ratio, a surplus of purine nucleotides stimulates pyrimidine synthesis, which in turn is inhibited by a surplus of pyrimidine nucleotides (Kantrowitz and Lipscomp 1990).

1.5.9.3 Aspartokinase

Aspartokinase I: homoserine dehydrogenase I from *Escherichia coli* catalyzes the first and the third step of the threonine biosynthesis pathway. Methionine biosynthesis controlled by an aspartokinase II: homoserine dehydrogenase II, and lysine biosynthesis regulated by an aspartokinase III, both branch off from this pathway. Aspartokinase I: homoserine dehydrogenase I consists of four identical subunits ($M_r=86\,000$). Each subunit has catalytic centers for both enzyme activities on two separate domains (*multifunctional enzyme*). The separate domains with their respective enzyme activities could be obtained by partial proteolysis or mutations. The aspartokinase domains retain their tetramer structure while homoserine dehydrogenase dissociates into dimers. In the native enzyme both activities are subject to end-product inhibition by threonine that shows a sigmoidal saturation pattern. This is more pronounced in the aspartokinase activity ($n_h \sim 4$) than in the homoserine dehydrogenase activity ($n_h \sim 3$). While the separate aspartokinase domain is still inhibited by threonine, the homoserine dehydrogenase domain becomes insensitive to this inhibition. Thus in the native enzyme both activities are regulated by one single regulatory binding site located on the aspartokinase domain. This was demonstrated by a one-step mutation where cooperativity for both activities was reduced by a comparable degree, i.e. to $n_h=1.65$ for aspartokinase and $n_h=1.45$ for homoserine dehydrogenase. It may be concluded from this that the native enzyme was formed by a fusion of the genes of two originally separate enzymes, an allosteric aspartokinase inhibited by threonine, and an originally unregulated homoserine dehydrogenase which was forced by fusion to adopt the allosteric properties.

1.5.9.4 Phosphofructokinase

Phosphofructokinase is the most important regulatory glycolyse enzyme. The corresponding reverse reaction step in gluconeogenesis is catalyzed by another enzyme, *fructose-1,6-bisphosphatase*. This necessitates a close regulatory linkage in order to avoid depletion of ATP by a *futile cycle* of the two counteracting reactions, the forward reaction consuming one ATP that cannot be regained in the reverse reaction. AMP is an activator of phosphofructokinase and an inhibitor of fructose-1,6-bisphosphatase. Phosphofructokinase, a tetramer enzyme, is inhibited by phosphoenolpyruvate, which stabilizes the T-state. The substrate fructose-6-phosphate exhibits a cooperative effect. The transition from T- to R-state is effected by a counter-rotation of 7° of each two dimers, respectively. The binding of the inhibitor AMP to the tetramer fructose-1,6-bisphosphatase causes a re-orientation of two dimers by 19° . In mammals both enzymes are additionally regulated by fructose-2,6-bisphosphate. The phosphofructokinase is allosterically activated and fructose-1,6-bisphosphatase is inhibited by negative cooperativity. Thus, both enzymes are subject to a reverse regulatory principle preventing a simultaneous parallel run of both reactions.

1.5.9.5 Allosteric Regulation of the Glycogen Metabolism

Biosynthesis and degradation of glycogen is also regulated by two allosteric enzymes. Here the allosteric control is additionally overlaid by a regulation by covalent modification, a phosphorylation governed by a cyclic cascade mechanism. *Glycogen synthase* is activated by glucose-6-phosphate and inhibited by AMP, while AMP activates and glucose-6-phosphate and ATP both inhibit the *glycogen phosphorylase*. The transition of glycogen phosphorylase from the T- to the R-state is accompanied by a relative rotation of the subunits against each other of 10° . The quaternary structure of the enzyme is modified towards a more favorable folding, the catalytic center moving into the vicinity of the allosteric AMP binding center and the phosphorylation site. This enzymatic active R-state is stabilized on the one hand by AMP and on the other hand by phosphate residues covalently bound at the phosphorylation site.

1.5.9.6 Membrane Bound Enzymes and Receptors

The *nicotinic acetylcholine receptor* was first described in fish electric organ (Heidmann and Changeux 1978). Five subunits arrange in a pentameric ring-like assembly in the order $\alpha 1$, γ , $\alpha 1$, δ , and $\beta 1$, i.e. 4 non-identical subunits, only $\alpha 1$ contributing two copies. All four non-identical subunits, however, possess high sequence homology, obviously emanating from a fourfold gene duplication, so that the pentameric structure can be regarded as pseudo-symmetrical with a five-fold rotational axis. The five subunits consist of three domains: the hydrophilic, extracellular N-terminal domain carries the neurotransmitter binding site, four membrane-spanning segments forming together a transmembrane channel, and a hydrophilic domain to the cytoplasmic site, which is susceptible to phos-

phorylation and transmits the signal obtained from the neurotransmitter site into the cell.

There exist only two binding sites with both $\alpha 1$ subunits and a γ , respectively, a δ subunit for acetylcholine. These are located at the boundary between the subunits, the acetylcholine binding domain consists of three loops of the α subunit and three loops of the γ or δ subunit, respectively. This is in contrast to the symmetry model where the number of binding sites is assumed to be equal to the protomer number and subject to the same symmetry conditions.

The *G-protein-coupled receptors* (GPCRs) are generally viewed as monomeric allosteric proteins. They consist of seven transmembrane α helices. The ligand binding site is located between the transmembrane helices or the extracellular domain. The intracellular loop and the C-terminal segment interact with the G-protein. The active forms of GPCRs occur as transmembrane oligomers (dimers or higher oligomers), e.g. functional chimeras between muscarinic and adrenergic receptors. Upon ligand binding dimerization may occur.

The microbial *tl-lipase* binds with high affinity to the membrane. The catalytic triad Asp, His, and Ser of the catalytic center is accessible from the surface only through a pocket with a lid. This closes reversibly the access to the active site. Fluorescence studies using a tryptophan in the lid-helix revealed a two-state model where an inactive closed-lid state ($K_d=350 \mu\text{M}$) and an active open-lid state ($K_d=53 \mu\text{M}$) could be discerned (Berg and Jain 2002).

1.6

Non-identical, Interacting Binding Sites

The description of the binding of ligands to identical, to non-identical independent, and to identical interacting binding sites should consequently be completed by the treatment of ligands binding to non-identical, interacting binding sites. However, such cases have not yet been convincingly identified. Hemoglobin may be such an example due to its α and β subunits, but because of their similar binding constants they behave like identical subunits. Different independent binding sites cause – as shown in Section 1.4 – a deviation from the normal binding pattern (Fig. 1.6) which is just opposite to positive cooperativity with identical interacting binding sites (Fig. 1.9), as can easily be seen from the double-reciprocal plots comparing Fig. 1.6 B and Fig. 1.11 B. With positive cooperativity the curve deviates to the upper right, with differing binding sites to the lower right. At comparable intensity both effects will compensate each other, resulting in a straight line as in normal binding patterns. Even at different intensities of both effects they will partially compensate one another and only the predominant mechanism can manifest itself in a weakened form. The same applies for the simultaneous existence of positive and negative cooperativity (e.g. if the initial binding step increases and the final one decreases the affinity), as the latter shows a similar curvature as binding to non-identical sites. The significance of such superpositions in the sense of a counter-regulation or fine tuning

may be discussed, incomplete compensations of counteracting effects may be responsible for inhomogeneities sometimes observed in saturation curves. In the absence of convincing examples, however, it remains open how far counteracting mechanisms within the same system actually exist.

On the other hand superposition of congeneric effects like negative cooperativity and binding to non-identical subunits will result in an amplification, but there are also no convincing examples.

References

Diffusion

- Berg, H. C. (1983) *Random Walks in Biology*, Princetown University Press, Princetown, New Jersey.
- Berg, O. G. (1985) Orientation constraints in diffusion-limited macromolecular association, *Biophys. J.* 47, 1–14.
- McCammon, J. A., Northrup, S. H. (1981) Gated binding of ligands to protein, *Nature* 293, 316–317.
- Noyes, R. M. (1961) Effects of diffusion rates in chemical kinetics, *Prog. React. Kinet.* 1, 129–160.

Binding Equilibria

- Adair, G. S. (1925) The hemoglobin system. The oxygen dissociation curve of haemoglobin, *J. Biol. Chem.* 63, 529–545.
- Klotz, I. M. (1985) Ligand-receptor interactions: facts and fantasies, *Quart. Rev. Biophys.* 18, 227–259.
- Langmuir, I. (1916) The constitution and fundamental properties of solids and liquids, *J. Am. Chem. Soc.* 38, 2221–2295.

Competition

- Thomä, N., Goody, R. S. (2003) What to do if there is no signal: using competition experiments to determine binding parameters, in: Johnson, K. A. *Kinetic Analysis of Macromolecules: A Practical Approach*, Oxford University Press, Oxford.

Graphic Methods

- Huang, C. Y. (1982) Determination of binding stoichiometry by the continuous varia-

tion method: The Job plot, *Methods Enzymol.* 87, 509–525.

- Job, P. (1928) Recherches sur la Formation de Complexes Minéraux en Solution, et sur leur Stabilité, *Ann. Chim. (Paris)* 9, 113–203.
- Klotz, I. M. (1946) The application of the law of mass action to binding by proteins. Interaction with calcium, *Arch. Biochem.* 9, 109–117.
- Rosenthal, H. R. (1967) A graphic method for determination and presentation of binding parameters in a complex system, *Anal. Biochem.* 20, 515–532.
- Scatchard, G. (1949) Attractions of proteins for small molecules and ions, *Ann. N. Y. Acad. Sci.* 51, 660–672.
- Stockell, A. (1959) The binding of diphosphopyridine nucleotide by yeast glyceraldehyde-3-phosphate dehydrogenase, *J. Biol. Chem.* 234, 1286–1292.
- Weder, H. G., Schildknecht, J., Lutz, L. A., Kesselring, P. (1974) Determination of binding parameters from Scatchard plots. Theoretical and practical considerations, *Eur. J. Biochem.* 42, 475–481.

Allosteric Enzymes, Cooperativity

- Berg, O. G., Jain, M. K. (2002) *Interfacial Enzyme Kinetics*, J. Wiley & Sons, Chichester.
- Bohr, C. (1904) Die Sauerstoffaufnahme des genuinen Blutfarbstoffes und des aus dem Blute dargestellten Hämoglobins, *Zentralblatt Physiol.* 23, 688–690.
- Changeux, J.-P., Edelstein, S. J. (2005) Allosteric mechanisms of signal transduction, *Science* 308, 1424–1428.

- Convay, A., Koshland, D.E. (1968) Negative cooperativity in enzyme action, *Biochemistry* 7, 4011–4023.
- Heidmann, T., Changeux, J.-P. (1978) Structural and functional properties of the acetylcholine receptor protein in its purified and membrane-bound states, *Ann. Rev. Biochem.* 47, 317–357.
- Hill, A.V. (1910) The possible effects of the aggregation of molecules of hemoglobin on its dissociation curves, *J. Physiol.* 40, iv–vii.
- Janin, J. (1973) The study of allosteric proteins, *Prog. Biophys. Mol. Biol.* 27, 77–120.
- Kantrowitz, E.R., Lipscomp, W.N. (1990) Aspartate transcarbamoylase: The molecular basis for a concerted allosteric transition, *Trends Biochem. Sci.* 15, 53–59.
- Koshland, D.E., Nemethy, G., Filmer, D. (1966) Comparison of experimental binding data and theoretical models in proteins containing subunits, *Biochemistry* 5, 365–385.
- Levitzki, A., Koshland, D.E. (1976) The role of negative cooperativity and half-of-the-sites reactivity in enzyme regulation, *Curr. Top. Cellular Reg.* 10, 1–40.
- Lipscomp, W.N. (1991) Structure and function of allosteric enzymes, *Chemtracts – Biochem. Mol. Biol.* 2, 1–15.
- Monod, J., Wyman, J., Changeux, J.-P. (1965) On the nature of allosteric transition: A plausible model, *J. Mol. Biol.* 12, 88–118.
- Neet, K.E. (1980) Cooperativity in enzyme function: Equilibrium and kinetic aspects, *Methods Enzymol.* 64, 139–192.
- Pauling, L. (1935) The oxygen equilibrium of hemoglobin and its structural interpretation, *Proc. Natl. Acad. Sci. USA* 21, 186–191.
- Perutz, M. (1970) Stereochemistry of cooperative effects in haemoglobin, *Nature* 228, 726–739.
- Perutz, M. (1990) *Mechanisms of Cooperativity and Allosteric Regulation in Proteins*, Cambridge University Press, Cambridge.
- Perutz, M., Wilkinson, A.J., Paoli, G., Dodson, G. (1998) *Annu. Rev. Biophys. Biomol. Struct.* 27, 1–34.
- Taketa, K., Pogell, B.N. (1965) Allosteric inhibition of rat liver fructose 1,6-diphosphatase by adenosine 5'-monophosphate, *J. Biol. Chem.* 240, 651–662.
- Viappiani, C., Bettati, S., Bruno, S., Ronda, L., Abbruzzetti, S., Mozzarelli, A., Eaton, W.A. (2004) New insight into allosteric mechanisms from trapping unstable protein conformations in silica gels, *Proc. Natl. Acad. Sci. USA* 101, 14414–14419.
- Wyman, J. (1967) Allosteric linkage, *J. Am. Chem. Soc.* 89, 2202–2218.
- Wyman, J., Gill, S.J. (1990) *Binding and Linkage*, University Science Books, Mill Valley, CA.
- Yonetani, T., Park, S., Tsuneshige, A., Imai, K., Kanaori, K. (2002) Global Allostery Model of Hemoglobin, *J. Biol. Chem.* 277, 34508–34520.